Mechanism of Drug Interaction between Valproic Acid and Carbapenem Antibiotics via Acylpeptide Hydrolase

2015

EIKO SUZUKI

TABLE OF CONTENTS

Page

Abbreviations

AANA	acetyl-alanine p-nitroanilide
APEH	acylpeptide hydrolase
AUC	area under the plasma concentration-time curve
BNPP	*bis*-*p*-nitrophenylphosphate
BSA	bovine serum albumin
C_{max}	the maximal plasma concentration
CYP	cytochrome P450
DDI	drug-drug interaction
DFP	diisopropyl fluorophosphate
DPD	dihydropyrimidine dehydrogenase
DRPM	doripenem
DTNB	5,5'-dithiobis(2-nitrobenzoic acid)
EDTA	ethylene diamine tetraacetic acid
5-FU	5-fluorouracil
IC_{50}	half maximal inhibitory concentration
IPI	International Protein Index
IS	internal standard
K_m	kinetic constant
LC/MS/MS	liquid chromatography-tandem mass spectrometry
LDH	lactate dehydrogenase
MEPM	meropenem
P450	cytochrome P450
PAPM	panipenem
PCMB	*p*-chloromercuribenzoic acid
PMSF	phenylmethylsulfonyl fluoride
pNPG	*p*-nitrophenyl β-glucuronide
SDS-PAGE	sodium dodecyl sulfate-polyacrylamide gel electrophoresis
$t_{1/2}$	terminal half-life
UDPGA	uridine 5'-diphosphoglucuronic acid
UGT	uridine 5'-diphospho-glucuronosyltransferase
VPA	valproic acid
VPA-G	valproic acid glucuronide
V_{max}	maximum velocity

General Introduction

Drug-drug interactions (DDIs) occur when one therapeutic agent either alters the concentration (pharmacokinetic interactions) or the biological effect of another agent (pharmacodynamic interactions) [1]. Pharmacokinetic DDIs can occur in processes of absorption, distribution, or clearance of the affected agent. Most clinical DDIs are relevant to metabolism, one of the clearance processes. In the metabolic process, adding a polar group or unmasking is mediated by drug-metabolizing enzymes to increase hydrophilicity of drugs for efficient elimination from the body. Although the majority of metabolism-mediated DDIs is related to inhibition or induction of cytochrome P450 (P450, CYP), one of the major drug-metabolizing enzyme clusters, there are a few cases of non P450 enzyme-related DDIs [2-4]. Of all, there was an unforgettable DDI mediated by dihydropyrimidine dehydrogenase (DPD), a non P450 enzyme [3]. DPD metabolizes 5-fluorouracil (5-FU), potent cancer chemotherapy drug. In Japan, it was found that concomitant use with sorivudine led to significant accumulation of 5-FU due to the inhibition of DPD by bromovinyluracil, a metabolite of sorivudine, followed by severe bone marrow depression and death. Later, sorivudine was withdrawn despite the effectiveness of its 20- to 100-fold lower dose for herpes zoster than acyclovir [5].

DDI potential of investigational drugs is evaluated using *in vitro* human samples and *in vivo* testing in animal species before clinical studies [6]. However, sometimes the prediction fails because *in vitro* findings do not always reflect the complexities of the whole human body and there are interspecies differences between human and animal *in vivo* systems. To overcome the problems, several research groups have developed chimeric mice, in which mouse liver is replaced by transplanted human liver cells [7-9]. Hasegawa et al. [7] have developed TK-NOG mice with humanized livers, which can sustain a high level of human engraftment over 8 months without special treatment other than a pathogen-free environment. The humanized liver in the chimeric mice expressed mRNAs encoding many human P450 enzymes, two uridine 5'-diphospho-glucuronosyltransferases (UGT), several transporters and transcription factors affecting drug metabolism at comparable levels to donor human hepatocytes, and exhibited the activity of CYP2D6, one of the major P450 enzymes involved in drug metabolism. In addition, the utility of this animal model to predict human drug metabolism and DDIs related to CYP3A has been suggested [10, 11]. Thus, TK-NOG chimeric mice with humanized livers appear to be a functional tool to predict clinical DDIs, at least mediated by P450 enzymes, as well as clarify the mechanisms of clinical DDIs.

Valproic acid (VPA), a simple, branched-chain fatty acid with a broad spectrum of anticonvulsant activity, is extensively used for treatment of various seizure types of epilepsy [12, 13]. Due to the versatility, VPA is often applied in combination with other antiepileptic agents [14]. Numerous types of DDIs between VPA and concomitantly used drugs including antiepileptic drugs have been reported [13], e.g., reduction in the plasma concentration of VPA by phenytoin or phenobarbital due to induction of hepatic drug-metabolizing enzymes [15]; enhanced VPA hepatotoxicity by phenytoin or carbamazepine due to the enhanced formation of 4-ene-VPA, a minor but toxic metabolite of VPA [16]; and inhibition of plasma protein binding of VPA by salicylic acid [15].

A clinically interesting DDI of VPA with carbapenem antibiotics has been reported [17, 18]. Carbapenem antibiotics have a broad spectrum of antibacterial activity both against Gram-positive and Gram-negative bacteria, and are used frequently in treating various infections [13, 19, 20]. While patients are receiving carbapenems, the plasma levels of VPA decrease below the narrow therapeutic window (50 – 100 μg/mL), resulting in the recurrence of epileptic seizures [17, 18]. In 1996, the contraindication for co-administration of these drugs was added to the Information on Adverse Reactions to Drugs from the Ministry of Health, Labour and Welfare in Japan, whereas in other countries a careful concomitant use is allowed and clinical interactions have still been reported [21-25].

The mechanism of this pharmacokinetic interaction has been studied by a number of researchers [26]. Some mechanisms related to absorption, distribution and metabolism of VPA have been proposed [13, 27-30]. Among them, metabolism in the liver has been considered to be the most important for interaction, as based on the following findings. VPA is mainly metabolized to the acylglucuronide (VPA-G) in the liver and subsequently excreted into bile and urine in rats. In hepatectomized rats, the interaction of VPA with carbapenems was not observed [13]. After treatment with panipenem (PAPM) to rats, the biliary excretion of VPA-G increased and the biliary excretion clearance did not change, suggesting that the formation of VPA-G was apparently accelerated. Although UGTs were not induced or activated by PAPM in rat liver microsomes, uridine 5'-diphosphoglucuronic acid (UDPGA) level was increased by 1.7 times, consistent with 1.8 times the increase of the apparent glucuronidation clearance of VPA [31]. However, VPA-G formation in monkey liver slice was increased 10 to 20 times by doripenem (DRPM), while the UDPGA level in the slice was increased only 1.4 times [29], suggesting that other processes contribute to the apparent acceleration in VPA-G formation. As one of the interaction processes, it is considered that the inhibition of the hydrolysis of VPA-G to VPA apparently accelerates the VPA-G formation. The hydrolysis of VPA-G was observed in rat and monkey liver homogenates [29]. The hydrolysis in rat liver cytosol was strongly inhibited by DRPM [29]. After intravenous administration of VPA-G to rats, the exposure of VPA in plasma was decreased by carbapenems, demonstrating that VPA-G hydrolysis and the inhibition by carbapenems also occur *in vivo* [29]. Collectively, VPA-G hydrolysis in the liver seems to be one of key processes for the interaction of VPA with carbapenems.

This thesis aims to clarify the mechanism of this interaction based on the hypothesis that the inhibition of reverse hydrolysis to VPA from VPA-G by carbapenems causes the rapid decrease in plasma VPA levels. In Chapter 1, a reverse hydrolase of VPA-G to VPA was successfully purified from human liver cytosol, where the VPA-G hydrolase activity is highly distributed. This enzyme was identified as APEH, and further *in vitro* studies revealed that APEH, but not β-glucuronidase, is exclusively involved in PAPM-sensitive VPA-G hydrolysis in human liver. APEH was considered to play a major role in this drug interaction via VPA-G hydrolysis.

Chapter 2 focuses on *in vivo* DDI evaluation after co-administration of VPA with MEPM to dogs and chimeric mice with humanized livers. In Section I, drug disposition and APEH activity after co-administration of VPA with MEPM to dogs were examined. More rapid decrease in plasma VPA

levels after administration with MEPM revealed that the drug interaction in dogs occurs in a similar manner to humans. *In vitro* characterization studies revealed that dog liver and kidney VPA-G hydrolase sensitive to carbapenems is cytosolic APEH, which is the same as in human liver. Increased urinary excretion of VPA-G and negligible hepatic and renal APEH activity at 24 h after dosing of MEPM, indicated long-lasting inhibition of APEH-mediated VPA-G hydrolysis by MEPM in dogs. Section II further examines the plausibility of the APEH-mediated DDI mechanism in TK-NOG chimeric mice with humanized livers, along with the capability of this animal model to evaluate DDI via non P450 enzyme.

Chapter 3 describes the inhibition mechanism of APEH by carbapenems. *In vitro* time-dependent inhibition and overnight dialysis studies revealed irreversible inhibition of APEH by carbapenems, consistent with the *in vivo* long-lasting inhibition of APEH after administration of MEPM in Chapter 2. Decreased binding of MEPM to APEH pretreated with a serine hydrolase inhibitor, diisopropyl fluorophosphates (DFP), primarily explains the irreversible inhibition by selective binding to the active serine of APEH. In this chapter, the chemical structure of carbapenems required for the inhibition was also examined by comparison with the open β-lactam ring form of MEPM and other classes of β-lactam antibiotics.

Chapter 1. Identification of VPA-G Hydrolase in Human Liver

1. Introduction

As the mechanism of interaction resulting in the decrease in plasma VPA level during concomitant use with carbapenems, the inhibition of reverse hydrolysis to VPA from VPA-G, the main metabolite of VPA has been suspected (**Fig. 1-1**). Liver, the main metabolic organ for VPA, has been considered to be the most important for this interaction since the interaction was not observed in hepatectomized rats [13].

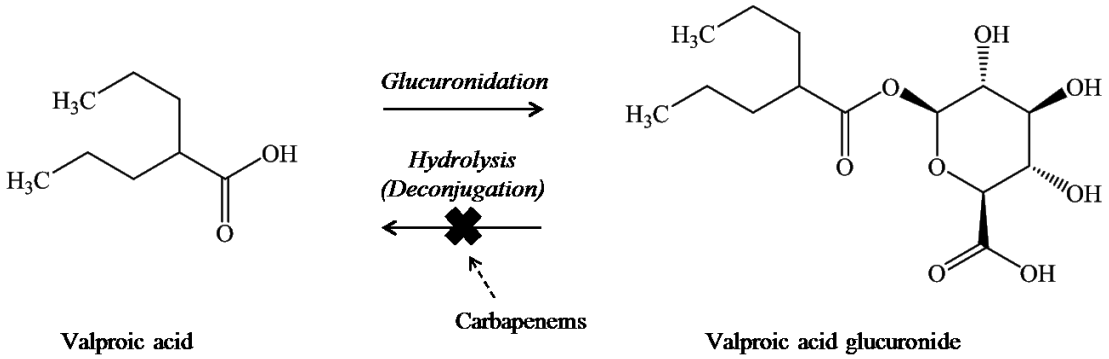

Figure 1-1. Possible mechanism of drug interaction of VPA with carbapenems.

In this chapter, the identification of VPA-G hydrolase from human liver cytosol, in which the hydrolase activity was highly located, is described. Using antiserum, the contribution of the identified enzyme to VPA-G hydrolysis was determined.

2. Results

2.1 VPA-G Hydrolase Activity in Human Liver Subcellular Fraction and Inhibition by PAPM

VPA-G hydrolase activity in human liver cytosol, microsomes, mitochondria and lysosomes at pH 7.4 are shown in **Fig. 1-2**. All the subcellular fractions showed hydrolase activity and cytosol had the highest activity. Lysosomes also showed the VPA-G hydrolase activity at pH 5. PAPM (0.03 mM) inhibited the VPA-G hydrolase activity in all the subcellular fractions, except for lysosomes at pH 5. The subcellular distribution of lactate dehydrogenase (LDH) activity, a marker enzyme of cytosol, was almost consistent with that of the VPA-G hydrolase activity (**Fig. 1-3**).

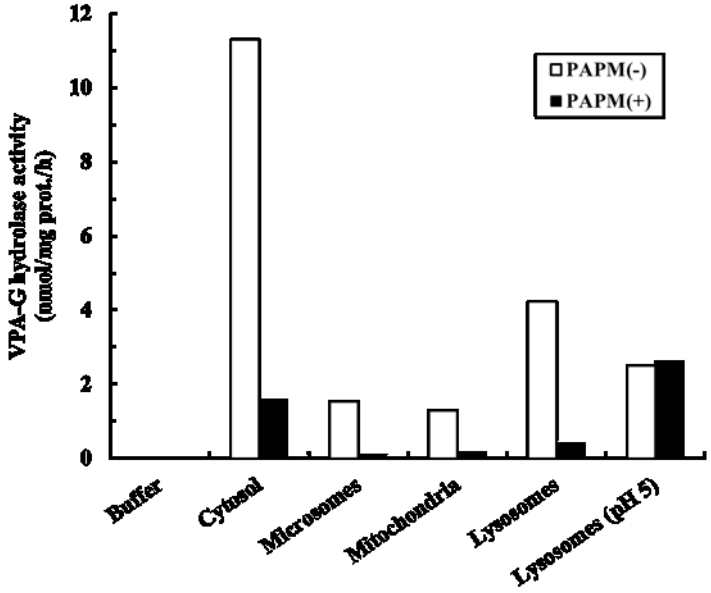

Figure 1-2. VPA-G hydrolase activity in human liver subcellular fractions. Subcellular fractions without indication of pH were tested at pH 7.4. Data represents the mean of duplicate determinations.

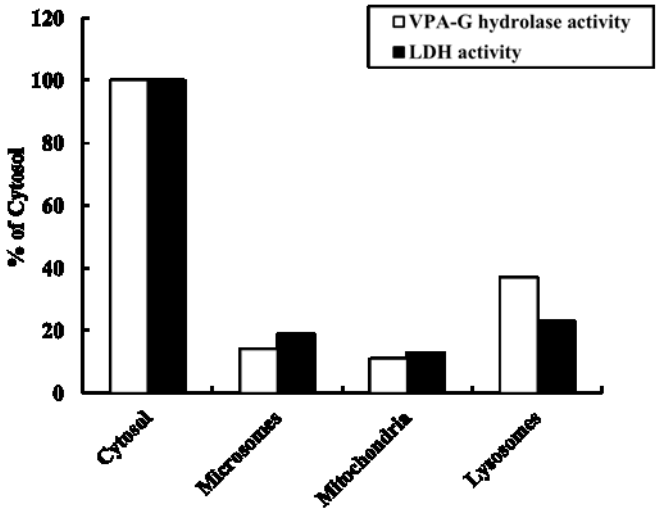

Figure 1-3. VPA-G hydrolase activity and LDH activity in human liver subcellular fractions at pH 7.4. Each activity is shown as % of cytosol. Data represents the mean of duplicate determinations.

2.2 VPA-G Hydrolysis by β-Glucuronidase

Because VPA-G hydrolysis is a deconjugation of glucuronide, the author examined the possibility of the hydrolysis by β-glucuronidase in cytosol. Saccharolactone, known as a β-glucuronidase inhibitor, decreased the hydrolytic activity in cytosol at pH 7.4 by 53.8% at 5 mM and abolished the activity at 25 mM (**Table 1-1**). However, commercially-available purified bovine liver β-glucuronidase hardly

hydrolyzed VPA-G at the same pH (0.710 pmol/Fishman unit/h). Since β-glucuronidase is mainly located in lysosomes, the activity of this enzyme at lysosomal pH was also tested. This enzyme showed greater activity at pH 5 (110 pmol/Fishman unit/h) than at pH 7.4. However, the hydrolase activity at pH 5 was not inhibited by PAPM even at 0.3 mM, which is 10 times higher than the inhibitory concentration in cytosol at pH 7.4. (**Table 1-2**).

Table 1-1. Residual VPA-G hydrolase activity in human liver cytosol (HLC) and recombinant human APEH (rhAPEH) at pH 7.4 after treatment with various inhibitors.

Typical target	Inhibitors	Conc. (mM)	Residual activity (%Control)	
			HLC	rhAPEH
β-Glucuronidase (APEH)	Saccharolactone	5	53.8	79.6
		25	0	17.4
Serine esterase	DFP	0.1	0	18.0
		1	0	18.0
Cholinesterase	Eserine	0.1	88.1	N.D.
		1	102.5	N.D.
Carboxylesterase	BNPP	0.1	110.2	N.D.
		1	85.6	N.D.
Esterase with SH-group	DTNB	1	19.4	29.6
		5	0	19.2
	PCMB	1	0	19.5
Metalloenzyme	EDTA	1	108.9	N.D.
		5	82.4	N.D.
Carbapenem-sensitive VPA-G hydrolase	PAPM	0.03	14.0	23.1

Data represents the mean of duplicate determinations. N.D., not determined.

Table 1-2. Residual VPA-G hydrolase activity of purified bovine liver β-glucuronidase at pH 5 after treatment with inhibitors.

Inhibitors	Conc. (mM)	Residual activity (%Control)
Saccharolactone	5	0
	25	0
PAPM	0.03	101.9
	0.3	101.0

Data represents the mean of duplicate determinations.

2.3 Inhibition of VPA-G Hydrolase Activity by Typical Esterase Inhibitors VPA-G Hydrolysis by β-Glucuronidase

Because VPA-G hydrolysis is a cleavage reaction of the carboxyl ester bond, the author examined

the possibility of the hydrolysis by typical esterases in cytosol. As shown in **Table 1-1**, DFP, a strong serine esterase inhibitor, completely inhibited the hydrolytic reaction at more than 0.1 mM. Eserine and *bis*-*p*-nitrophenylphosphate (BNPP), a specific inhibitor for cholinesterase and carboxylesterase, showed little or no inhibition of the hydrolysis, respectively. 5,5'-Dithiobis(2-nitrobenzoic acid) (DTNB) and *p*-chloromercuribenzoic acid (PCMB), known as inhibitors of esterase containing SH-groups, completely inhibited the hydrolysis at 5 and 1 mM, respectively. The inhibitory effect of ethylene diamine tetraacetic acid (EDTA), a chelate agent, was very weak.

2.4 Purification of VPA-G Hydrolase from Human Liver Cytosol

The author tried to purify VPA-G hydrolase(s) from human liver cytosol by anion exchange chromatography and hydroxyapatite affinity chromatography. The active fractions were subjected to sodium dodecyl sulfate-polyacrylamide gel electrophoresis (SDS-PAGE) and a thick band was found at 75 kDa (**Fig. 1-4**). The 75-kDa protein band was digested with trypsin within the gel and the resulting peptides were extracted and sequenced by liquid chromatography-tandem mass spectrometry (LC/MS/MS). The MS/MS spectra data were searched against a composite target/decoy International Protein Index (IPI) human database using Mascot software. As a result, the 75-kDa protein was identified as APEH (IPI accession number: IPI00337741) with a sequence coverage of 71% (**Table 1-3**).

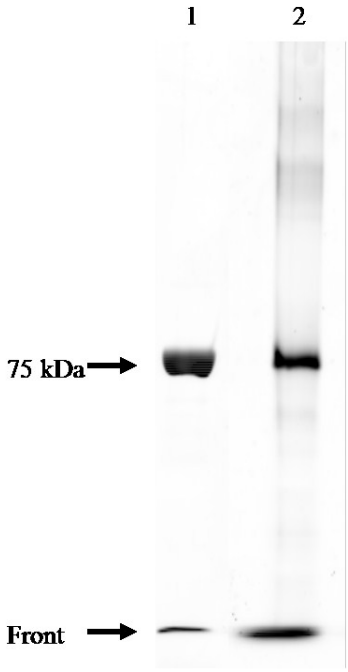

Figure 1-4. SDS-PAGE of VPA-G hydrolase purified from human liver cytosol. Lane 1, molecular mass marker; lane 2, purified VPA-G hydrolase. The gel was revealed by silver staining.

Table 1-3. Correspondence of tryptic peptides of a 75 kDa protein purified from human liver cytosol to human APEH (IPI accession number: IPI00337741).

Peptide Sequence	Localization of peptide in APEH sequence	Mascot Score
ERQVLLSEPEEAAALYR	2-18	79
QVLLSEPEEAAALYR	4-18	71
QPALSAACLGPEVTTQYGGQYR	23-44	83
TVHTEWTQR	45-53	45
TVHTEWTQRDLER	45-57	20
QYLVFHDGDSVVFAGPAGNSVETR	66-89	114
GELLSRESPSGTMK	90-103	49
ESPSGTMKAVLR	96-107	54
KAGGTGPGEEKQFLEVWEK	108-126	32
QFLEVWEKNRK	119-129	45
KLKSFNLSALEK	129-140	49
LKSFNLSALEK	130-140	53
SFNLSALEK	132-140	53
HGPVYEDDCFGCLSWSHSETHLLYVAEK	141-168	87
AESFFQTKALDVSASDDEIAR	173-193	52
AESFFQTK	173-180	49
ALDVSASDDEIAR	181-193	83
LKKPDQAIKGDQFVFYEDWGENMVSK	194-219	87
LKKPDQAIK	194-202	40
GDQFVFYEDWGENMVSK [a]	203-219	99
RSALYYVDLIGGK	279-291	70
SALYYVDLIGGK	280-291	87
CELLSDDSLAVSSPR	292-306	118
IVYLQYPSLIPHHQCSQLCLYDWYTK	314-339	65
VTSVVVDVVPR	340-350	64
QLGENFSGIYCSLLPLGCWSADSQR	351-375	71
VVFDSAQR	376-383	55
SRQDLFAVDTQVGTVTSLTAGGSGGSWK	384-411	120
QDLFAVDTQVGTVTSLTAGGSGGSWK	386-411	143
LLTIDQDLMVAQFSTPSLPPTLK [a]	412-434	98
VGFLPSAGKEQSVLWVSLEEAEPIPDIHWGIR	435-466	77
VGFLPSAGK	435-443	48
EQSVLWVSLEEAEPIPDIHWGIR	444-466	85
VLQPPPEQENVQYAGLDFEAILLQPGSPPDK	467-497	51
TQVPMVVMPHGGPHSSFVTAWMLFPAMLCK	498-527	53
MGFAVLLVNYR [a]	528-538	77
GSTGFGQDSILSLPGNVGHQDVK	539-561	75
TPLLLMLGQEDR [a]	665-676	112
TPLLLMLGQEDRR	665-677	49
RVPFKQGMEYYR	677-688	29
STHALSEVEVESDSFMNAVLWLR	705-727	115

Sequence coverage is 71%. [a] Methionine in the peptides is identified as the oxidized form.

2.5 Inhibitory Effect of PAPM and Esterase Inhibitors on the VPA-G Hydrolytic Activity of Recombinant APEH

The construct of human APEH (derived from IOH3679, Matching nucleotide accession number: NM_001640.3, Invitrogen) with FLAG tag was transfected in FreeStyle 293F cells and the resulting protein was purified using the affinity tag and two-step column chromatography. Then, the inhibitory effect of PAPM and esterase inhibitors on the VPA-G hydrolytic activity of the recombinant human APEH was examined. As shown in **Table 1-1**, PAPM significantly inhibited the hydrolase activity of the recombinant APEH at 0.03 mM. The effect of DFP, DTNB, PCMB and saccharolactone on the recombinant APEH was similar to human liver cytosol as well.

2.6 Immunodepletion of APEH by Rabbit Anti-human APEH Antiserum

To examine the contribution ratio of APEH to VPA-G hydrolysis in human liver cytosol, rabbit anti-human APEH antibody was raised by multiple injections of recombinant human APEH. The resultant antiserum showed a binding ability to APEH protein but it could not inhibit the APEH activity (data not shown), therefore, the author used an immunodepletion method. Human liver cytosol was treated with the antiserum to deplete APEH. Western blot analysis revealed that APEH was successfully depleted in the resulting cytosol (**Fig. 1-5a**). The APEH depleted cytosol completely lacked the VPA-G hydrolase activity, whereas cytosol treated with preimmune serum kept 97% of the control activity (**Fig. 1-5b**). Similarly, acetyl-alanine *p*-nitroanilide (AANA), a typical substrate of APEH, was hardly hydrolyzed in APEH depleted cytosol (**Fig. 1-5b**). In contrast, cytosolic β-glucuronidase activity, measured as *p*-nitrophenyl β-glucuronide (pNPG) activity, was not affected by depletion of APEH at pH 5 (**Fig. 1-5b**). Neither cytosol treated with anti-APEH antiserum, preimmune serum, nor buffer showed β-glucuronidase activity at pH 7.4.

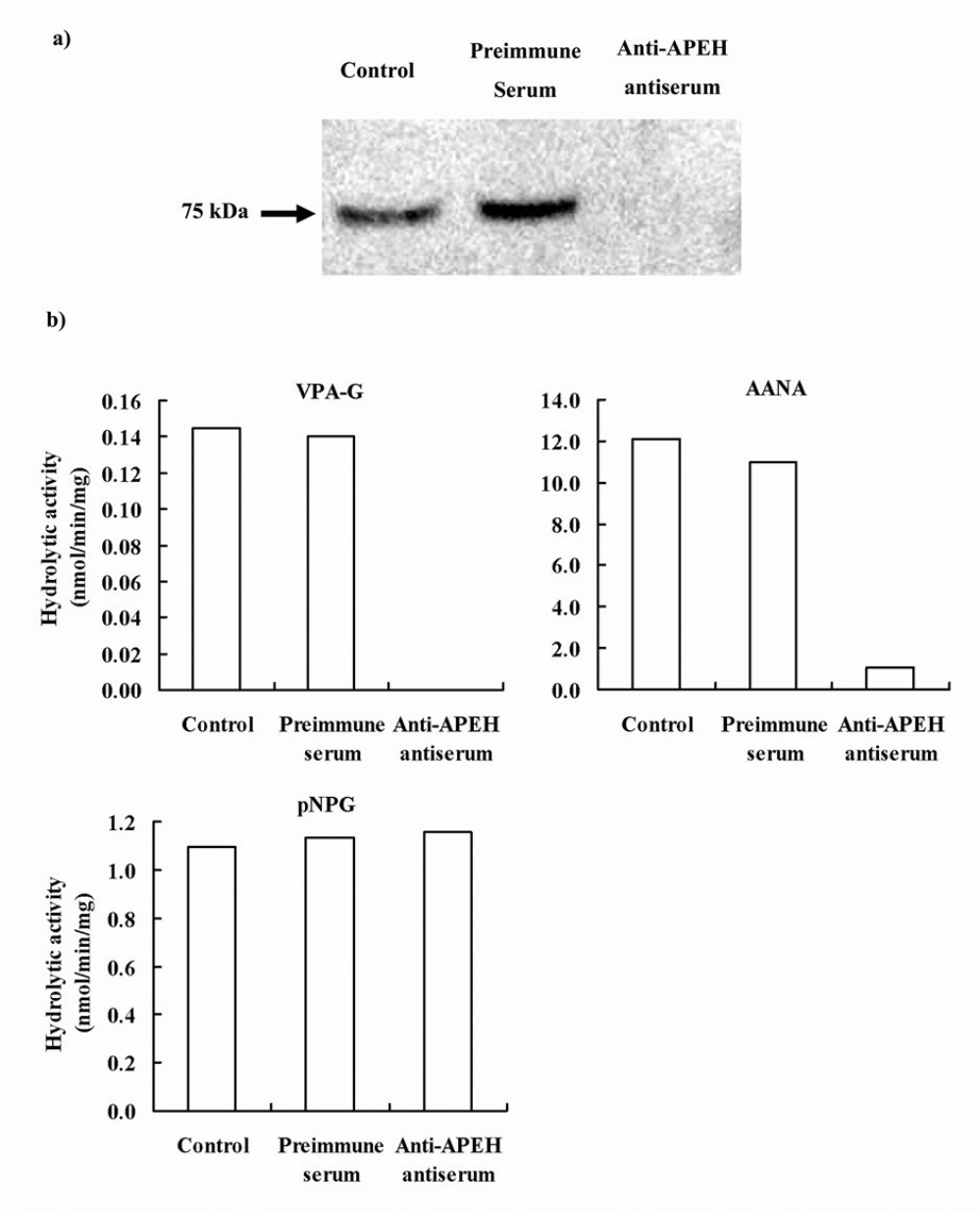

Figure 1-5. APEH depletion (a) and various hydrolytic activity (b) in human liver cytosol after treatment with preimmune serum and anti-human APEH antiserum. Immunodepleted samples prepared in duplicate. One sample each was subjected to Western blot analysis. Hydrolytic activity is shown as the mean value or the value of the pooled sample. The cytosol treated with buffer is shown as the control.

3. Discussion

First the localization of VPA-G hydrolase in the liver to determine a target fraction for the hydrolase identification was examined (**Fig. 1-2**). The highest hydrolase activity was found in cytosol at neutral pH. The VPA-G hydrolase activity at the same pH in the other fractions, such as microsomes,

mitochondria and lysosomes was considered to be contaminated fraction of cytosol since the activity of these fractions was almost in parallel with the activity of LDH, which is the marker enzyme for cytosol (**Fig. 1-3**). Lysosomes also showed VPA-G hydrolase activity at acidic pH, which is optimal condition for lysosomal enzymes (**Fig. 1-2**). An inhibition experiment by PAPM revealed that cytosolic VPA-G hydrolase activity at neutral pH is PAPM-sensitive, but lysosomal activity at acidic pH is insensitive. Thus, VPA-G hydrolase, subjected to inhibition by PAPM, is mainly located in cytosol.

From human liver cytosol, a single enzyme with a molecular weight of 75 kDa as a VPA-G hydrolase was purified (**Fig. 1-4**). This enzyme was identified as APEH, a serine peptidase. The chemical inhibition profiles of the recombinant human APEH by PAPM and enzyme inhibitors (DFP, DTNB, PCMB and saccharolactone) was similar to that of human liver cytosol (**Table 1-1**). Human liver cytosol from which APEH is removed by anti-APEH antiserum completely abolished the corresponding 75 kDa-protein and VPA-G hydrolytic activity (**Fig. 1-5**). These results demonstrate that APEH is a single enzyme involved in PAPM-sensitive VPA-G hydrolysis in human liver cytosol.

The exclusive involvement of APEH to cytosolic VPA-G hydrolysis is also supported by the following findings. Minor or no contribution of cholinesterase, carboxylesterase and metalloenzyme to cytosolic VPA-G hydrolysis is suggested by little or no effect on the VPA-G hydrolysis by either cholinesterase inhibitor (eserine), carboxylesterase inhibitor (BNPP) or metalloenzyme inhibitor (EDTA), as shown in **Table 1-1**. Interestingly, involvement of β-glucuronidase in cytosolic VPA-G hydrolysis is considered to be negligible, since APEH depleted cytosol completely lacked VPA-G hydrolase activity without any loss of pNPG β-glucuronidase activity and purified bovine liver β-glucuronidase hardly hydrolyzed VPA-G at cytosolic pH (**Table 1-3** and **Fig. 1-5**). In contrast, Nakamura et al. [32] had concluded that VPA-G is hydrolyzed by β-glucuronidase other than serine esterase(s) in cytosol based on the inhibition profile that the VPA-G hydrolase activity was inhibited by saccharolactone, a β-glucuronidase inhibitor, but not by phenylmethylsulfonyl fluoride (PMSF), a serine esterase inhibitor. However, this profile is corresponding to that of APEH reported previously [33]. Thus, all the findings suggest the contribution of cytosolic APEH to the hydrolysis. This is an example that hydrolase, but not β-glucuronidase, is the major enzyme which catalyzes the deconjugation of acylglucuronide.

APEH (EC 3.4.19.1) is known as a cytosolic serine peptidase, which consists of four identical monomers with a molecular weight of 75 kDa. It catalyzes the hydrolysis of N-acylated peptide to an acylamino acid and a peptide with a free N-terminus [34]. The physiological role of APEH is considered as a regulation of the turnover and function of proteins because it has been reported that the acylation of proteins is related to the stability, function and interaction with other proteins. Other than N-acylated peptides, APEH also hydrolyzes simple esters such as p-nitrophenyl esters [35]. This is the first report to show the involvement of APEH in drug metabolism.

APEH has been found in various tissues including the kidney, intestine and erythrocytes as well as the liver [36]. Therefore, the possibility cannot be ruled out that APEH in other tissues contributes to the interaction of VPA with carbapenems via VPA-G hydrolysis. At least, renal APEH may contribute to the DDI since increase in urinary excretion of VPA-G was observed in rabbits after co-administration with

MEPM without significant change of the plasma VPA-G concentration-time profile [37]. VPA glucuronidation activity in the human liver and kidney microsomes is very similar [38] and the VPA-G hydrolase activities in both tissues are also comparable (data not shown). As the total activity in the liver is considered to be greater than that in the kidney because of the difference of the blood flow and total protein between both tissues, hepatic APEH could play a major role for this DDI via VPA-G hydrolysis.

4. Short Summary

In summary, cytosolic APEH is a single PAPM-sensitive VPA-G hydrolase in human liver. This work presents that APEH is involved in drug metabolism for the first time.

Chapter 2. Drug Disposition and APEH Activity after Administration of VPA with MEPM in Dogs and Chimeric Mice with Humanized Livers

Chapter 2 focuses on *in vivo* DDI evaluation after co-administration of VPA with MEPM to dogs and chimeric mice with humanized livers. This chapter consists of the following two sections. Section I describes VPA and VPA-G dispositions after administration of VPA with MEPM to dogs. Also *in vitro* characterization of dog VPA-G hydrolase, which is identified as the dog counterpart of APEH, and *ex vivo* APEH activity in dog biopsy samples after administration of MEPM were examined. Section II describes *in vivo* DDI studies in chimeric mice with humanized livers and the utility of this animal model for evaluation of non P450-related DDI is discussed.

I. VPA and VPA-G Disposition and APEH Activity after Administration of VPA with MEPM in Dogs and *In vitro* Studies to Identify Dog VPA-G Hydrolase

1. Introduction

The inhibition of reverse hydrolysis to VPA from VPA-G by carbapenems is considered to play a key role for the DDI of VPA with carbapenems. In Chapter 1, a reverse hydrolase of VPA-G to VPA was successfully purified from human liver cytosol, where the VPA-G hydrolase activity is highly distributed. This enzyme was identified as APEH, and further *in vitro* studies revealed that APEH, but not β-glucuronidase, is exclusively involved in PAPM-sensitive VPA-G hydrolysis in human liver.

Section I intends to clarify the relevance of APEH-mediated VPA-G hydrolysis *in vivo* through determination of *ex vivo* APEH activity in dog biopsy samples, and the disposition of VPA and VPA-G after co-administration of VPA with MEPM. In parallel, *in vitro* characterization of APEH as dog VPA-G hydrolase was carried out.

2. Results

2.1 VPA and VPA-G in Plasma, Urine, and Bile after Intravenous Administration of VPA and MEPM to Dogs

After administration of VPA with MEPM, terminal half-life ($t_{1/2}$) was shorter than that after dosing of VPA only (**Fig. 2-1** and **Table 2-1**). Plasma clearance of VPA increased after co-administration with MEPM. Urinary excretion of VPA-G increased from 1 h after administration of VPA in the MEPM-treatment group and the total urinary excretion (0 – 6 h) was 1.5-fold higher than the control group (**Table 2-2**). The plasma level and bile excretion of VPA-G showed no change (**Fig. 2-1**, **Table 2-1** and **Table 2-2**). VPA was negligible in the urine and bile after co-administration with or without MEPM.

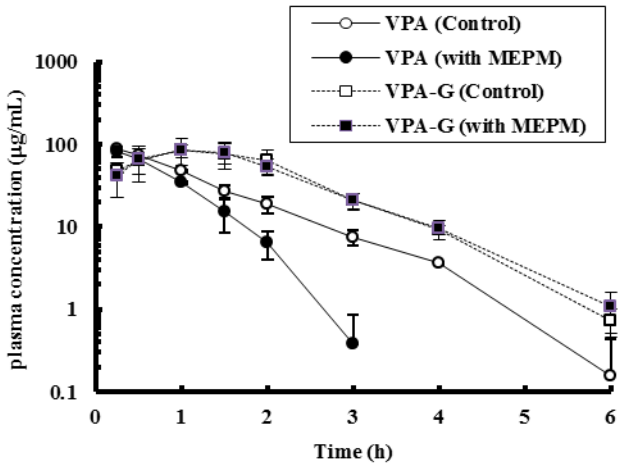

Figure 2-1. Plasma concentration-time profiles of VPA and VPA-G after intravenous administration of VPA (30 mg/kg) with or without MEPM (100 mg/kg) to three dogs. Each value represents mean ± SD.

Table 2-1. Pharmacokinetic parameters after intravenous administration of VPA (30 mg/kg) with or without MEPM (100 mg/kg) to three dogs.

Parameter	VPA		VPA-G	
	VPA + Saline	*VPA + MEPM*	*VPA + Saline*	*VPA + MEPM*
$AUC_{0\text{-}6h}$ (μg·h/ml)	127 ± 10	87.2 ± 4.2	199 ± 59	193 ± 41
$t_{1/2}$ (h)	0.76 ± 0.03	0.33 ± 0.07	0.59 ± 0.08	0.7 ± 0.16
CL (ml/h/kg)	237 ± 17	344 ± 17	-	-
V_{ss} (ml)	262 ± 15	227 ± 33	-	-
t_{max} (h)	-	-	1.0 ± 0.0	1.2 ± 0.3
C_{max} (μg/ml)	-	-	86.1 ± 31.3	85.2 ± 17.4

Each value represents mean ± SD.

Table 2-2. Urinary and biliary excretion of VPA-G after intravenous administration of VPA (30 mg/kg) with or without MEPM (100 mg/kg) to three dogs.

	Excretion ratio (%)	
	Urine	*Bile*
VPA + Saline		
0-1 h	14.1 ± 2.5	8.4 ± 1.1
1-2 h	16.4 ± 1.8	5.3 ± 0.5
2-4 h	11.0 ± 5.5	5.9 ± 1.5
4-6 h	7.6 ± 6.9	0.7 ± 0.2
Total	49.1 ± 13.1	20.3 ± 1.7
VPA + MEPM		
0-1 h	12.2 ± 9.9	9.5 ± 3.9
1-2 h	30.6 ± 10.4	10.9 ± 5.3
2-4 h	25.7 ± 3.3	4.5 ± 1.7
4-6 h	5.1 ± 3.6	1.2 ± 1.4
Total	73.6 ± 13.4	26.1 ± 7.9

Each value represents mean ± SD.

2.2 Identification of a VPA-G Hydrolase in Dog Liver and Kidney

To confirm the location of a VPA-G hydrolase, VPA-G hydrolase activity in dog liver and renal subcellular fraction was measured. The highest VPA-G hydrolase activity was found in the cytosol at pH 7.4 both in the liver and kidney (**Fig. 2-2**). The activity was inhibited by PAPM and MEPM (**Fig. 2-2**). Although the hydrolase activity was observed in lysosomes at pH 5, it was not affected by the carbapenems (**Fig. 2-2**).

The sensitivity of the VPA-G hydrolase in dog liver and renal cytosol to esterase inhibitors was examined. The VPA-G hydrolase activity in both cytosolic fractions was completely inhibited by DFP (0.1 and 1 mM) and PCMB (1 mM) and was partially affected by DTNB (1 mM) and saccharolactone (5 mM) (**Fig. 2-3**).

To examine the contribution ratio of APEH to VPA-G hydrolysis, APEH-depleted dog liver and renal cytosol by an immunodepletion method using rabbit anti-APEH antiserum was prepared. The APEH depleted cytosol completely lacked the VPA-G hydrolase activity, whereas the cytosol treated with preimmune serum showed almost the same activity as the control (**Fig. 2-4**). Similarly, AANA, a typical substrate of APEH, was hardly hydrolyzed in the APEH depleted cytosol (**Fig. 2-4**). In contrast, cytosolic β-glucuronidase activity, measured as pNPG activity, was not affected by depletion of APEH at pH 5 (**Fig. 2-4**). Either the cytosol treated with anti-APEH antiserum, preimmune serum, or buffer showed a negligible β-glucuronidase activity at pH 7.4.

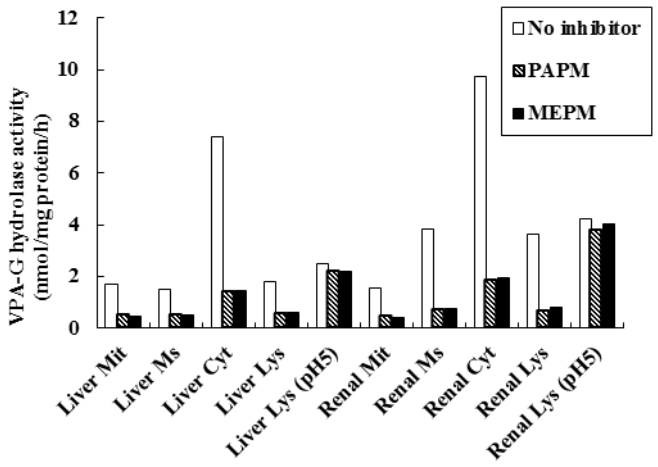

Figure 2-2. VPA-G hydrolase activity in dog liver and renal subcellular fractions. Data represents the mean of duplicate determinations. Subcellular fractions without indication of pH were tested at pH 7.4.

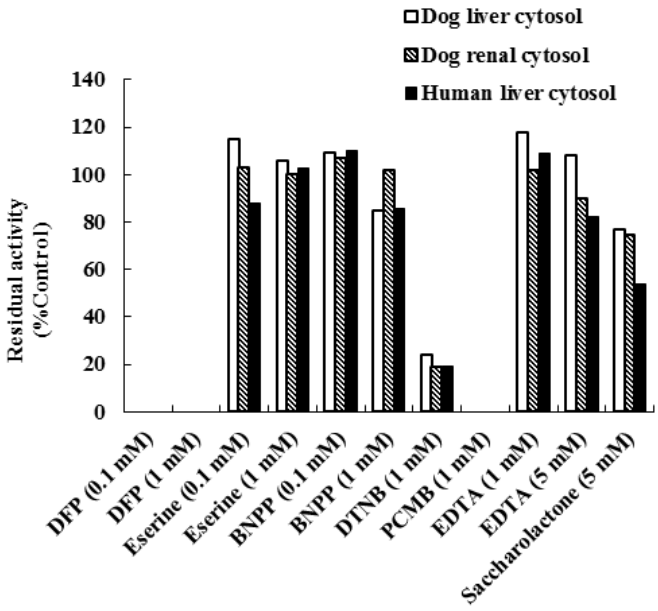

Figure 2-3. Residual VPA-G hydrolase activity in dog liver and renal cytosol at pH 7.4 after treatment with various inhibitors. Data represents the mean of duplicate determinations. Data from human liver cytosol was reported in Chapter 1.

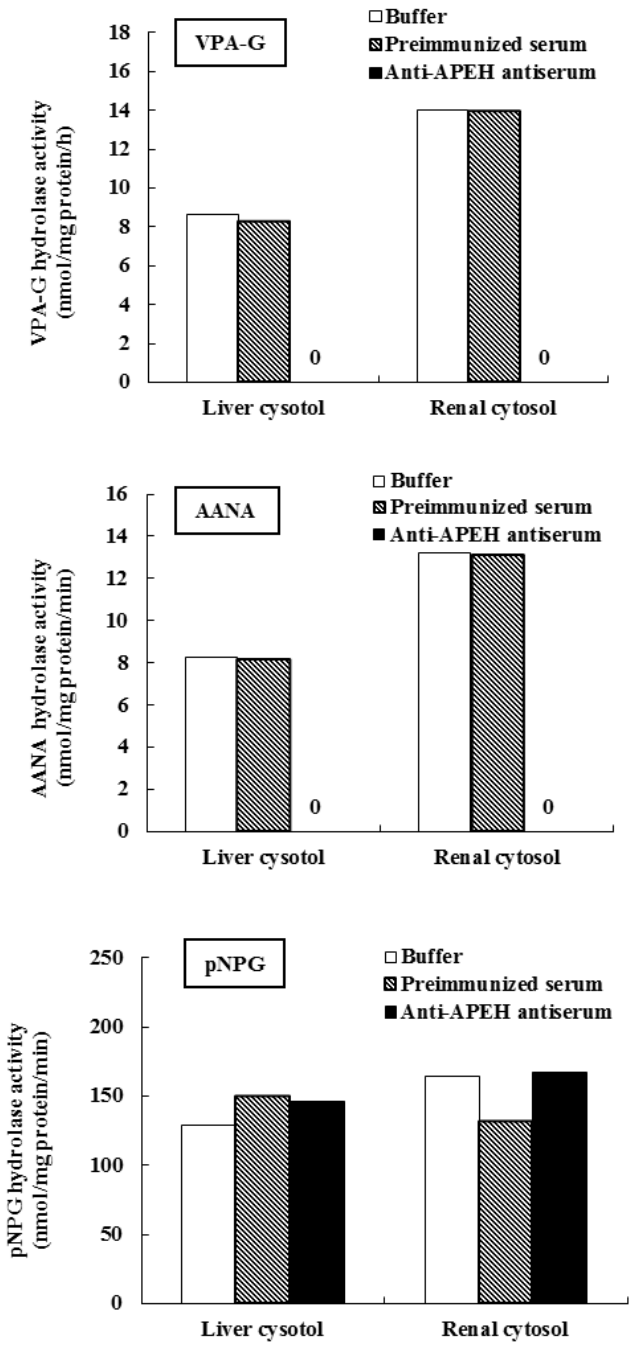

Figure 2-4. Various hydrolytic activity in dog liver and renal cytosol after treatment with buffer, preimmune serum and anti-human APEH antiserum. Immunodepleted samples prepared in duplicate. Data is shown as the mean value.

2.3 APEH Activity in Dog Liver and Kidney after Co-administration with MEPM

APEH activity measured as AANA hydrolase activity in the liver and renal S9 prepared from biopsy samples after administration of VPA with MEPM to a dog was negligible (**Fig. 2-5**).

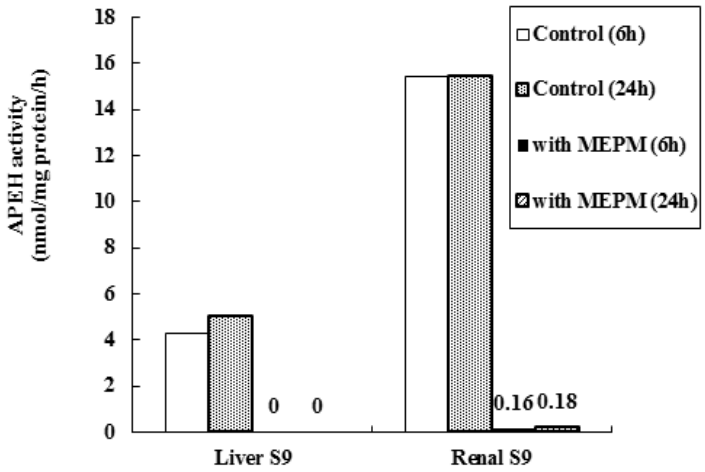

Figure 2-5. APEH activity in dog liver and renal S9 after intravenous administration of VPA (30 mg/kg) with or without MEPM (100 mg/kg) to a dog. S9 was prepared from biopsy samples obtained at 6 h and 24 h after the administration.

3. Discussion

Plasma concentrations of VPA after administration of VPA and MEPM to dogs decreased more rapidly than after administration of VPA only (**Fig. 2-1** and **Table 2-1**), demonstrating that the drug interaction of VPA with MEPM was also observed in dogs. Urinary/biliary excretion of VPA itself was negligible in both groups after co-administration with and without MEPM, whereas increased urinary excretion of VPA-G was observed after co-administration with MEPM (**Table 2-2**), suggesting that VPA-G hydrolysis was inhibited by MEPM in dogs. Increased plasma clearance of VPA after co-administration with MEPM also suggests an interruption of VPA supply from VPA-G by MEPM.

Dog APEH was identified to be a VPA-G hydrolase through the examination of the subcellular location and characterization using both inhibitors and anti-APEH antiserum. The highest VPA-G hydrolase activity was found in cytosol from both the liver and kidney at neutral pH and was inhibited by PAPM and MEPM (**Fig. 2-2**). The hydrolase activity was also found in lysosomes at acidic pH and was not changed by PAPM and MEPM (**Fig. 2-2**). Thus, dog VPA-G hydrolase, subjected to inhibition by carbapenems, is mainly located in cytosol in both the liver and kidney. The inhibition profile of the VPA-G hydrolase activity in both dog liver and renal cytosol (**Fig. 2-3**) was quite similar to that of human liver cytosol and recombinant human APEH in Chapter 1. APEH-depleted dog liver and renal cytosol prepared by immunodepletion using anti-APEH antiserum completely lacked the VPA-G hydrolytic activity as well as AANA, a typical substrate of APEH (**Fig. 2-4**). β-Glucuronidase activity (pNPG hydrolase activity) was not changed by the depletion of APEH (**Fig. 2-4**). These results demonstrate that APEH is a single VPA-G hydrolase in dog liver and renal cytosol as well as in humans.

APEH activity was negligible in dog liver and kidney samples after co-administration with MEPM and the lack of *in vivo* APEH activity was maintained until 24 h (**Fig. 2-5**). This is the first observation of the inhibition of APEH activity by a carbapenem under the *in vivo* condition. The long-lasting inhibition

of dog APEH was consistent with clinical findings that the plasma VPA level after discontinuation of a carbapenem remained low for several days [21-25]. These findings suggest that APEH activity is also sustainably inhibited by carbapenems in clinical settings, contributing to the rapid decrease of plasma VPA levels in the case of concomitant use of both drugs. The inhibition of renal APEH and increased urinary excretion of VPA-G by MEPM suggested that renal inhibition of hydrolysis to VPA from VPA-G also caused the decrease of VPA supply to plasma after renal uptake of VPA-G. Further studies to investigate the renal disposition of VPA and VPA-G are required to confirm the contribution of inhibition of renal APEH to decrease plasma VPA levels.

4. Short summary

In summary, the DDI of VPA with carbapenems in dogs is caused by long-lasting inhibition of VPA-G hydrolysis mediated by APEH, resulting in rapid decrease in plasma VPA levels and increase in urinary excretion of VPA-G, suggesting the clinical importance of APEH-mediated VPA-G hydrolysis in the DDI mechanism. This work presents the inhibition of APEH activity by a carbapenem under the *in vivo* condition for the first time. This work also suggests the utility of animal *in vivo* models combined with *in vitro* assays to identify involved enzyme(s) for better understanding of DDI mechanisms.

II. VPA and VPA-G Disposition and APEH Activity after Administration of VPA with MEPM in Chimeric Mice with Humanized Livers

1. Introduction

Chimeric mice carrying humanized livers have received increased attention as a tool to evaluate clinical feasibility of DDI [6, 10]. A TK-NOG mouse with humanized liver is one of the chimeric animal models and two researches showed the capability to predict clinical feasibility of P450-related DDI in the TK-NOG chimeric mice [10, 11].

Chapter 1 and Section I in this chapter revealed that APEH is dog and human VPA-G hydrolase, and long-lasting inhibition of APEH-mediated VPA-G hydrolysis causes the DDI of VPA with carbapenems in dogs. In Section II, VPA and VPA-G disposition and APEH activity in TK-NOG chimeric mice with humanized livers were examined after co-administration with MEPM in order to determine the capability of this animal model for prediction of clinical DDIs mediated by a non-P450 enzyme, and plausibility of the APEH-mediated DDI mechanism.

2. Results

2.1 VPA and VPA-G in Plasma and Urine after Intravenous Administration of VPA and MEPM to Chimeric Mice

Plasma VPA and VPA-G concentration-time profiles and respective pharmacokinetic parameters after administration of VPA with or without MEPM to chimeric mice with humanized livers and normal TK-NOG mice are shown in **Fig. 2-6** and **Table 2-3**. After administration of VPA, $t_{1/2}$ of plasma VPA concentration in chimeric mice was prolonged compared with normal mice. After administration of VPA with MEPM to chimeric mice, plasma VPA decreased with shorter $t_{1/2}$ than that after dosing of VPA only. Area under the plasma concentration-time curve (AUC) and urinary excretion of VPA-G in the MEPM-treatment chimeric mice were 2.7-fold and 1.4-fold higher than the control chimeric mice (**Table 2-3** and **Table 2-4**).

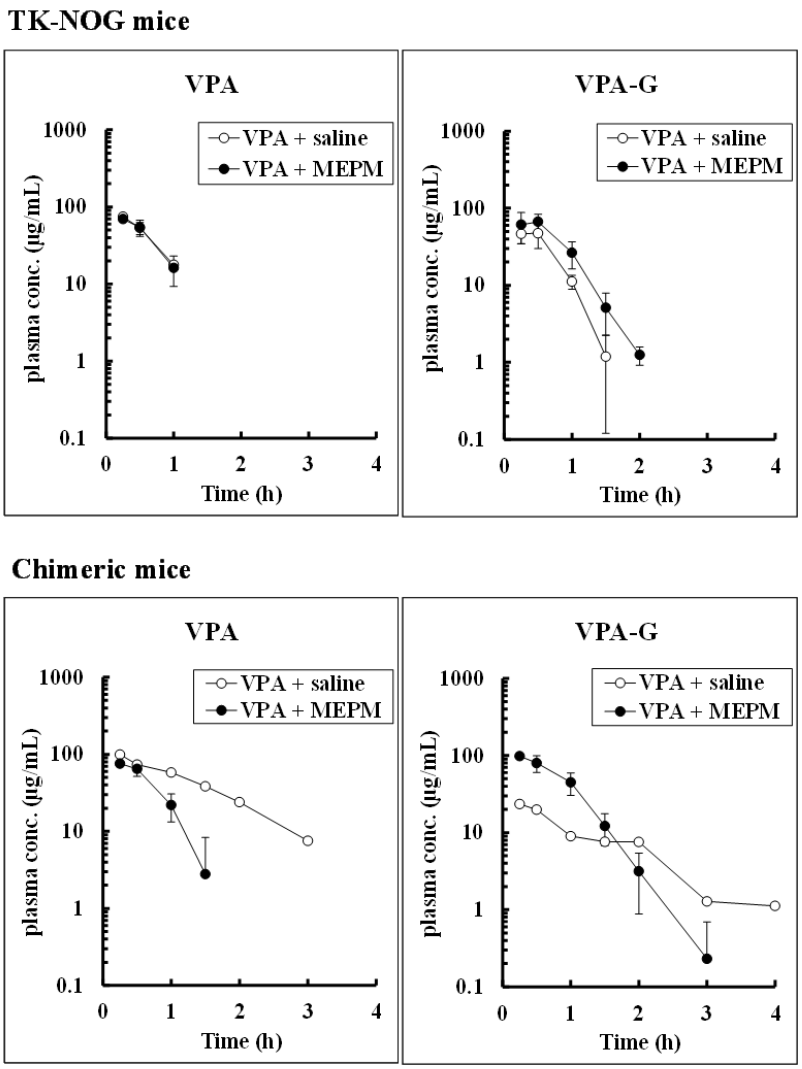

Figure 2-6. Plasma concentration-time profiles of VPA and VPA-G after intravenous administration of VPA (30 mg/kg) with or without MEPM (125 mg/kg) to chimeric mice with humanized livers and TK-NOG mice. Data is shown as mean ± SD (N=3-4) except for VPA + saline group of chimeric mice, shown as mean (N=2). Data at 0.25 h after dosing in VPA + MEPM group of chimeric mice is shown as mean (N=2).

Table 2-3. Pharmacokinetic parameters of VPA and VPA-G after intravenous administration of VPA (30 mg/kg) with or without MEPM (125 mg/kg) to chimeric mice with humanized livers and TK-NOG mice.

Parameter	TK-NOG mice		Chimeric mice	
	VPA + saline	*VPA + MEPM*	*VPA + saline* †	*VPA + MEPM* ‡
VPA				
AUC_{0-4h} (μg·h/mL)	61.2 ± 2.6	57.4 ± 7.3	142.8	82.9 ± 25.6
$T_{1/2}$ (h)	0.35 ± 0.02	0.35 ± 0.09	0.82	0.4 ± 0.05
CL (mL/h/kg)	456 ± 17	494 ± 85	199	397 ± 114
Vss (mL/kg)	228 ± 34	241 ± 25	228	182 ± 69
VPA-G				
AUC_{0-4h} (μg·h/mL)	35.6 ± 8.5	57.0 ± 9.8	29.1	77.4 ± 27.4
$T_{1/2}$ (h)	0.22*	0.23 ± 0.01	0.87	0.69 ± 0.90
Tmax (h)	0.42 ± 0.14	0.33 ± 0.14	0.25	0.44 ± 0.13
Cmax (μg/mL)	51.7 ± 13.7	67.7 ± 17.5	23.5	80.8 ± 20.8

Parameters are shown as mean ± SD (N=3). *Parameter is from one animal because it cannot be calculated from other two animals. †The group consisted of two animals. ‡The group consisted of four animals.

Table 2-4. Urinary excretion of VPA-G for 0-24 h after intravenous administration of VPA (30 mg/kg) with or without MEPM (125 mg/kg) to chimeric mice with humanized liver and TK-NOG mice.

Parameter	TK-NOG mice		Chimeric mice	
	VPA + saline	*VPA + MEPM*	*VPA + saline*	*VPA + MEPM*
Urinary excretion (%dose)	21.6 ± 9.9	42.8 ± 22.4	40.2 ± 6.0	55.4 ± 30.0

Data is shown as mean ± SD (N=3).

2.2 APEH Activity in Humanized Liver and Mouse Kidney Homogenates after Co-administration with MEPM

APEH activity measured as AANA hydrolase activity in humanized liver and mouse kidney homogenates collected at 24 h after co-administration with MEPM to chimeric mice was decreased by 75.4% and 31.4% of control, respectively (**Table. 2-5**).

Table 2-5. APEH activity in the liver and kidney homogenate at 24 h after intravenous administration of VPA (30 mg/kg) with or without MEPM (125 mg/kg) to chimeric mice with humanized livers and TK-NOG mice.

Homogenate	APEH activity (nmol/min/mg)			
	TK-NOG mice		Chimeric mice	
	VPA + saline	*VPA + MEPM*	*VPA + saline*	*VPA + MEPM*
Liver	9.26 ± 5.61	3.07 ± 0.37	17.0 ± 5.0	4.19 ± 0.98
Kidney	12.8 ± 3.4	10.7*	12.5 ± 2.1	8.57 ± 1.25

*Data is shown as mean of two samples, which are a sample derived from one animal and a mixture of tissues from two animals (erroneously mixed).

3. Discussion

Human *in vitro* and dog *in vitro/in vivo* findings in Chapter 1 and Section I in this chapter strongly suggest that inhibition of APEH-mediated VPA-G hydrolysis by carbapenems causes rapid decrease in plasma VPA levels below the therapeutic window. However, APEH inhibition in clinical settings was unclarified. TK-NOG chimeric mice with humanized liver, which is subjected to transplantation of normal human hepatocytes to their liver injured by ganciclovir treatment, have received increased attention as a functional tool to expect clinical pharmacokinetics/toxicity in recent years [7, 39, 40]. In this section, in order to examine the capability of this animal model for prediction of non P450-related DDIs and plausibility of the APEH-mediated mechanism in the DDI of VPA with carbapenems, *in vivo* APEH activity as well as VPA and VPA-G dispositions after co-administration of VPA with MEPM to the chimeric mice were investigated.

After co-administration with MEPM to the chimeric mice, $t_{1/2}$ of plasma VPA was shorter than that after administration of VPA only (0.82 h and 0.35 h), suggesting that the DDI of VPA with MEPM occurs in chimeric mice in the same manner as in dogs and in clinical settings (**Fig. 2-6** and **Table 2-3**). The DDI could not occur in normal TK-NOG mice. This is the first example showing the capability to evaluate a non P450-related DDI in chimeric mice.

Terminal half-life of plasma VPA in the chimeric mice did not reach that of *ca*. 12 h in clinical settings. This discrepancy is possibly explained by the interspecies difference in VPA glucuronidation activity. VPA glucuronidation activity by UGT in mouse-derived tissues including survived mouse liver cells in humanized livers in the chimeric mice may be higher than that in human tissues. Plasma $t_{1/2}$ of VPA in mice, rats, dogs and cynomolgus monkeys is much shorter than the clinical parameter, (**Table 2-3**, Section I in this chapter) [13, 29]. Furthermore, VPA-G concentration in human plasma is very low compared with those animals (**Fig. 2-6**, Section I in this chapter) [13, 29, 41]. These findings suggest that the VPA-G formation rate in humans is small. Although kinetic parameters of VPA-G formation in mouse and monkey liver microsomes are not available, VPA-G formation clearance determined using human liver microsomes is lower than that of rat, or dog liver microsomes [31, 38]. The interspecies difference in APEH activity may less impact the VPA clearance since APEH activity in rat, dog and human liver cytosol was comparable (Chapter 1, Section I in this chapter and unpublished data). Hence, such an

interspecies difference of metabolism between humanized liver and mouse cells may limit quantitative use, however, this animal model could be useful to examine qualitative clinical feasibility of a DDI and its mechanism.

In the chimeric mice, decrease in APEH activity in the humanized liver and intact mouse kidney, and increase in AUC and urinary excretion of VPA-G were observed (**Table 2-3**, **Table 2-4** and **Table 2-5**), indicating that inhibition of APEH-mediated VPA-G hydrolysis by carbapenems causes the DDI of VPA with carbapenems in the chimeric mice as well as in dogs (Section I in this chapter). This is the first observation to suggest that human APEH activity is inhibited by MEPM *in vivo*. While renal APEH activity was equal both in normal and chimeric mice and was weakly inhibited by MEPM, the DDI occurred only in chimeric mice. These results indicate that hepatic APEH in humanized liver contributes to the longer $t_{1/2}$ of plasma VPA level in the chimeric mice by more effective recycling of VPA from VPA-G compared to normal mice, suggesting the importance of hepatic APEH in the clinical DDI as well.

The inhibition of APEH-mediated VPA-G hydrolysis by carbapenems is considered to be the most plausible mechanism for the interaction in humans and animals in common, based on the following findings. The significant increase of VPA-G formation in rat, monkey and human liver materials *in vitro* after incubation of VPA with carbapenems and increased excretion of VPA-G in rats, dogs and chimeric mice with humanized livers *in vivo* after co-administration of VPA with carbapenems were observed (Chapter 1 and this chapter) [29, 42]. Neither induction nor activation of UGT by PAPM was observed in rat *in vitro* and *in vivo* examinations [31]. VPA-G hydrolysis to VPA after administration of VPA-G to rats was inhibited by co-administration with carbapenems [29]. APEH was identified to be dog and human VPA-G hydrolase sensitive to carbapenems, and *in vivo* inhibition of APEH activity by MEPM in dogs and chimeric mice with humanized livers was found along with increased excretion of VPA-G and the rapid decrease of plasma VPA levels in Chapter 1 and this chapter. Collectively, the inhibition of APEH-mediated VPA-G hydrolysis is observed as the acceleration of VPA-G formation, resulting in the increased excretion of VPA-G and rapid decrease of VPA in plasma. In contrast, the other 3 proposed mechanisms, namely, 1) interaction in the intestinal absorption process, 2) interaction in the enterohepatic circulation process, and 3) interaction in the blood cell distribution process [26], are less likely in humans than the interaction in the VPA-G hydrolysis process. Torii et al. [28] reported that the maximal plasma concentration (C_{max}) and AUC of VPA was decreased by 50 – 60% after oral administration of VPA with treatment of imipenem and PAPM to rats, suggesting that the intestinal absorption of VPA might be inhibited by carbapenems. However, the plasma level of VPA was also decreased at later time points, even after intravenous administration of VPA with the carbapenems [28]. In a case report of a Chinese patient who received 800 mg of VPA (p.o., once daily), the plasma concentration of VPA was decreased from 39 μg/mL to 10 μg/mL after MEPM treatment (1 g, i.v., twice daily) and it was not improved by the change of the dose regimens of VPA (400 mg i.v. and 1200 mg p.o., once daily) and MEPM (0.5 g i.v., twice daily) [25]. These findings indicate that the interaction of VPA and carbapenems occur after intravenous administration of VPA as well as after the oral administration, and the inhibition of intestinal absorption of VPA would not be significant in rats and humans. Kojima et al. [27] reported that the

decrease of VPA in plasma was not observed after intravenous administration of VPA and PAPM to bile duct-cannulated rats, suggesting that carbapenems excreted into bile may suppress the enterohepatic recirculation of VPA by killing intestinal flora, which deconjugates VPA-G in gut. However, this result has been controversial because the other report showed that the interaction occurred in bile duct-cannulated rats [13]. In addition, the biliary concentrations of carbapenems in humans are less than that of other β-lactam antibiotics, which can also kill intestinal flora and have been reported not to interact with VPA [18, 43-47], supporting that the interaction in the enterohepatic circulation process would be improbable in humans. As to the blood cell distribution process, Omoda et al. [30] reported that the blood levels of VPA were not changed when the plasma level was decreased after intravenous administration of VPA with carbapenems in rats. However, both the blood and plasma levels of VPA were decreased in patients [30], therefore, this mechanism does not contribute to the interaction in humans. Thus, the inhibition of VPA-G hydrolysis in the liver is the most plausible mechanism of the interaction of VPA with carbapenems in humans at present.

4. Short summary

In summary, this is the first example to show the capability of chimeric mice with humanized livers as a functional tool for evaluation of DDIs via non P450 enzymes. In the same manner as in dogs, in chimeric mice with humanized livers, the DDI of VPA with carbapenems is caused by long-lasting inhibition of APEH-mediated VPA-G hydrolysis, resulting in a rapid decrease in plasma VPA level and increase in urinary excretion of VPA-G. These results obtained in this chapter strongly support that this APEH inhibition is the most plausible mechanism for the clinical DDI of VPA with carbapenems and hepatic APEH is the major contributor to the DDI.

Chapter 3. The Long-lasting Inhibition Mechanism of APEH by Carbapenems: *In Vitro* Studies using Human Liver Cytosol and Purified Porcine APEH with a Similar Property to Its Human Counterpart

1. Introduction

Chapter 3 describes the inhibition mechanism of APEH by carbapenems. Chapter 2 reveals that long-lasting inhibition of VPA-G hydrolysis mediated by APEH causes the DDI of VPA with MEPM in dogs and chimeric mice with humanized liver. In Chapter 3, the inhibition mechanism of APEH by carbapenems was investigated focusing on reversibility, the site of action on the enzyme and the important structure of carbapenems comparing to its open β-lactam ring form (**Fig 3-1**) and other class of β-lactam antibiotics. Human liver cytosol and purified porcine APEH with a similar property to its human counterpart were used as APEH enzyme sources in this chapter.

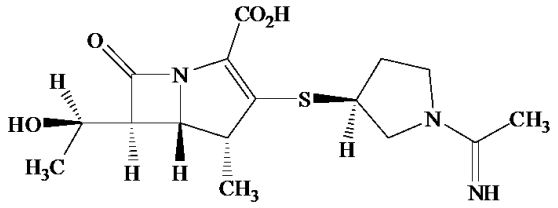

PAPM

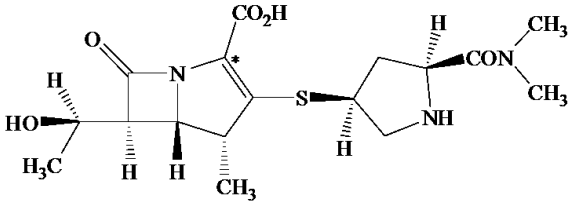

MEPM

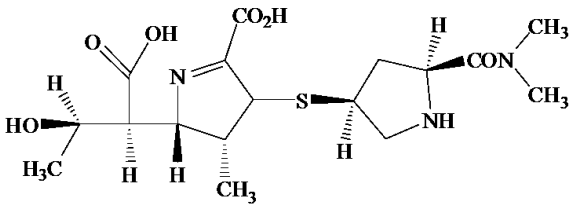

Open β-lactam ring form of MEPM

Figure 3-1. Chemical structures of PAPM, MEPM and open β-lactam ring form of MEPM.
* ^{14}C-labeled position of ^{14}C-MEPM used in Chapter 3. 4.

2. Results

2.1 Kinetic Parameters of VPA-G Hydrolytic Activity of APEH in Human Liver Cytosol and Purified Porcine Liver APEH

K_m and V_{max} values of the VPA-G hydrolytic activity in human liver cytosol and purified porcine liver APEH were calculated to be 3.06 μM and 0.238 nmol/min/mg protein, and 7.83 μM and 253 nmol/min/mg protein, respectively.

2.2 Preincubation Time-dependency of Inhibition of APEH by Carbapenems

At a substrate concentration of 3 μM (approximately equal to K_m), both PAPM and MEPM inhibited APEH in human liver cytosol without preincubation and half maximal inhibitory concentration (IC_{50}) values were 1.77 and 3.50 μM, respectively. The inhibitory effect was enhanced approximately 20-fold after preincubation for 30 min (**Table 3-1**).

Table 3-1. Preincubation time-dependency of inhibitory effect of PAPM and MEPM on APEH in human liver cytosol.

Carbapenem	Preincubation time (min)	IC_{50} (μM)
PAPM	0	1.77
	10	0.231
	30	0.0857
MEPM	0	3.5
	10	0.41
	30	0.161

IC_{50} values were calculated from the mean of duplicate determinations at each test concentration.

2.3 Effect of Dialysis on Interaction between Porcine APEH and MEPM

Because of the comparable K_m, the similar inhibition profiles by typical hydrolase inhibitors (data not shown) and 92% identity of amino acid sequence [48], purified porcine APEH was used in this experiment instead of the human counterpart. Porcine APEH was dialyzed after incubation with or without MEPM and the VPA-G hydrolytic activity was measured. Before dialysis, APEH activity incubated with MEPM decreased to 10.5% of that without MEPM. After overnight dialysis, the activity of APEH incubated with MEPM was not recovered (6.2% of activity without MEPM treatment). The remaining binding ratio of ^{14}C-labeled MEPM to APEH after overnight dialysis was 61.2%, whereas the binding ratio of ^{14}C-MEPM to bovine serum albumin (BSA) was 6.3% (**Table 3-2**). After preincubation of APEH with DFP, the binding ratio of ^{14}C-MEPM to APEH decreased to 12.1% (**Table 3-2**). The binding ratio of ^{14}C-MEPM to BSA did not change by DFP treatment (**Table 3-2**).

Table 3-2. Inhibitory effect of DFP on the binding of MEPM to purified porcine APEH and BSA.

Protein	DFP	Binding ratio (%)
APEH	−	61.2 ± 2.2
	+	12.1 ± 1.5
BSA	−	6.3 ± 0.7
	+	6.6 ± 0.4

Data represent the mean ± S.D. of triplicate determinations.

2.4 Inhibitory Effect of Open β-Lactam Ring Form of MEPM and Other β-Lactam Antibiotics on APEH

The open β-lactam ring form of MEPM did not show the inhibitory effect on APEH activity in human liver cytosol even at 100 μM. Likewise, other β-lactam antibiotics, which have a different ring structure adjacent to the β-lactam ring compared with carbapenems and various lengths of the side chains, did not inhibit the APEH activity (**Table 3-3**).

Table 3-3. Inhibitory effect of β-lactam antibiotics on acylpeptide hydrolase in human liver cytosol.

β-Lactam antibiotic	Chemical structure	Concentration (μM)	Residual activity (%)
Clavulanic acid	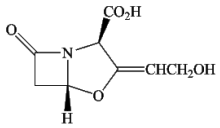	2	107.2
		20	103.6
		200	101.8
6-Aminopenicillanic acid	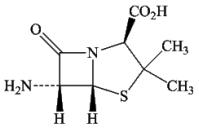	2	96.4
		20	95.5
		200	97.3
Benzylpenicillin	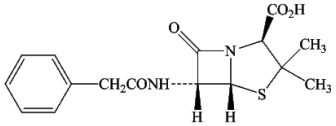	2	100.0
		20	95.5
		200	106.3
Ampicillin	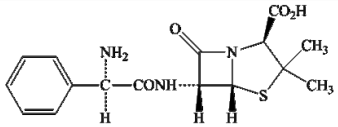	2	97.3
		20	99.1
		200	118.9
Meropenem	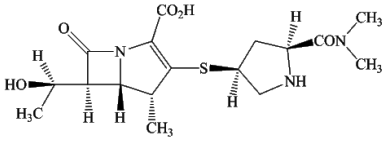	2	23.5
		20	3.2
		200	2.3

Data represent the mean of duplicate determinations.

3. Discussion

The author examined the inhibition characteristics of VPA-G hydrolase activity of APEH by carbapenems, which would lead to a decrease in the plasma concentration of VPA. PAPM and MEPM inhibited APEH in human liver cytosol with 1.70 and 3.50 μM of IC_{50}, respectively. These values are clinically relevant because the C_{max} values of PAPM and MEPM in humans were around 70 – 160 μM [19].

The inhibitory effect of the carbapenems on APEH was dependent on the preincubation time. After preincubation with carbapenems for 30 min, PAPM and MEPM showed smaller IC_{50} (0.0857 and 0.161 μM, respectively, **Table 3-1**). A similar preincubation time-dependency was also confirmed in the previous report [49]. Thus, carbapenems inhibit APEH irreversibly. In addition, these observations are consistent with long-lasting inhibition of APEH in the dog and humanized chimeric mice in Chapter 2 and the delayed recovery of plasma VPA levels in clinical conditions [21-25]. In contrast, the open β-lactam ring form of MEPM did not affect APEH activity even at 100 μM, indicating that the inhibition of APEH by carbapenems requires the closed β-lactam ring structure.

To further characterize the irreversible inhibition mechanism, the dialytic effect on APEH after incubation with MEPM was examined. The activity of purified porcine APEH decreased by 89.5% and it did not recover after overnight dialysis (93.8% inhibition), also demonstrating that the inhibition was irreversible. The binding ratio of MEPM to APEH after dialysis was 61.2% (**Table 3-2**), suggesting that the inhibition of APEH by MEPM is primarily explained by strong binding of MEPM to the enzyme. The difference between the inhibitory effect of APEH activity by MEPM (93.8%) and the binding ratio (61.2%) after dialysis is unclarified. However, the structural modification in the active site of some APEH enzyme molecules might occur when leaving MEPM fragment, resulting in enzyme inactivation, as seen in the inhibition mechanism of class A serine β-lactamase by clavulanic acid [50]. By preincubation of APEH with DFP, the binding ratio of MEPM to APEH decreased to 12.1%. DFP is known to inhibit serine hydrolases such as APEH by covalently binding to the active serine of enzymes [51]. Thus, the irreversible inhibition mechanism of carbapenems would be primarily explained by binding to the active serine of APEH. In addition, low binding ratio of MEPM to BSA was not changed by DFP (**Table 3-2**), suggesting that the binding of MEPM to APEH is selective.

Despite the binding selectivity to APEH, a little portion of MEPM also bound to BSA. It might have been caused by the high reactivity of the β-lactam ring of carbapenems. After administration of biapenem to rats, an amide metabolite with the open β-lactam ring structure was observed in plasma and urine [52]. This metabolite seems to be produced by a nonenzymatic nucleophilic attack to the carbonyl carbon of the closed β-lactam ring by the amino group of cystine, since mixing biapenem with amino acid infusions containing cystine (and also cysteine) leads to the degradation of biapenem, as stated in the Japanese package insert of biapenem. As for thienamycin (the primary carbapenem) and MEPM, a similar reaction with cysteine has been reported [53, 54]. Thus, the β-lactam ring of carbapenems could have some reactivity to proteins.

The proposed irreversible inhibition mechanism of APEH by carbapenems, that is, the binding to

the active serine of APEH, resembles that of antibacterial activity. The β-lactam ring attacks the active serine in penicillin binding proteins, which is needed for the last step of cell wall production in bacteria, resulting in the formation of a stable ester bond with the open β-lactam ring structure [55, 56]. Although this pharmacological function is considered to be common among all the β-lactam antibiotics such as penicillins and cephems, they have not been reported to interact with VPA. This may be caused by the following structural differences: 1) the heterocyclic structure adjacent to β-lactam ring, 2) the length of side chain attached to β-lactam ring, 3) the relative configuration of the side chain. Unique five-membered non-heterocycle ring structure and/or relative configuration of the side chain of carbapenem structure could contribute to the inhibition potential because clavulanic acid and three penicillins did not inhibit APEH (**Table 3-3**). The small side chain attached to carbapenem β-lactam ring was considered to enable the β-lactam ring to readily attack the active serine of APEH. However, no inhibition by clavulanic acid with no side chain and 6-aminopenicillanic acid with an amino group suggests that the small side chain is unrelated to the APEH inhibition.

Regarding the binding of carbapenems to the active serine of APEH, the author cannot rule out the possibility that carbapenems inhibit other serine esterases involved in drug metabolism, such as carboxylesterase and cholinesterase. However, there are no articles reporting the interactions between carbapenems and ester drugs hydrolyzed by those esterases (such as angiotensin converting enzyme inhibitors) thus far. Therefore, carbapenems are unlikely to affect other serine esterase activities in clinical practice.

4. Short summary

In summary, carbapenems irreversibly inhibit APEH. To exert the inhibitory effect, the closed β-lactam ring structure is essential and other unique structures of carbapenems would contribute to the inhibition. The inhibition mechanism is primarily explained by selective binding to the active serine of APEH.

Summary

This thesis has investigated the mechanism of the DDI between VPA and carbapenems, based on the hypothesis that the inhibition of reverse hydrolysis to VPA from VPA-G by carbapenems causes the rapid decrease in plasma VPA levels. The author identified VPA-G hydrolase as APEH, and examined *in vivo* inhibition of this hydrolase by carbapenems in dogs and chimeric mice with humanized livers, and the mechanism of inhibition using *in vitro* biological sources. New findings provided from the present research are described in the following.

Chapter 1 describes the identification of VPA-G hydrolase in human liver, which is considered to be a key molecule to maintain plasma VPA levels via VPA-G hydrolysis. The highest VPA-G hydrolase activity was found in human liver cytosol at neutral pH. The cytosolic VPA-G hydrolase was inhibited by DFP and PAPM, but not BNPP and eserine, suggesting that PAPM-sensitive VPA-G hydrolase in cytosol was serine hydrolase, but not well-known serine esterases, namely, carboxylesterase and cholinesterase. Through successive column chromatography, the cytosolic VPA-G hydrolase was identified as APEH, serine peptidase. This is the first study to find an involvement of APEH in drug metabolism. The chemical inhibition profile of recombinant human APEH by enzyme inhibitors was quite similar to that of cytosolic VPA-G hydrolase. APEH-depleted cytosol, prepared by an immunodepletion method using anti-APEH serum, completely abolished the activity to hydrolyze VPA-G and the typical substrate of APEH. Lysosomal and cytosolic β-glucuronidase is unrelated to PAPM-sensitive VPA-G hydrolysis. These findings indicate that cytosolic APEH exclusively catalyzes PAPM-sensitive VPA-G hydrolysis in human liver. These findings also provide an example that hydrolase, but not β-glucuronidase, is a major enzyme which catalyzes the deconjugation of acylglucuronide.

Chapter 2 describes the examination of the inhibition of APEH-mediated VPA-G hydrolysis and the resulting change in the dispositions of VPA and VPA-G after co-administration of VPA with MEPM in animals. In Section I, an examination of the drug disposition and APEH activity in dog *in vivo*, along with identification of dog VPA-G hydrolase, was carried out. A more rapid decrease in plasma VPA levels after co-administration with MEPM revealed that the drug interaction in dogs occurs in the same manner as clinical settings. Increased urinary excretion of VPA-G and plasma clearance of VPA after co-administration with MEPM suggest that inhibition of VPA-G hydrolysis by MEPM causes an interruption of the VPA supply into plasma from VPA-G hydrolysis, resulting in accelerated urinary excretion of VPA-G. The accelerated urinary excretion of VPA-G also suggests the involvement of a renal enzyme in VPA-G hydrolysis. Dog VPA-G hydrolase in the liver and kidney was identified as cytosolic APEH through the examination of the subcellular location and characterization using both inhibitors and anti-APEH antiserum. The highest dog VPA-G hydrolase activity was found in cytosol from the liver and kidney. The inhibition profile of the cytosolic VPA-G hydrolase activity in the dog liver and kidney by chemical inhibitors including PAPM and MEPM was quite similar to that of the human liver cytosol and recombinant human APEH in Chapter 1. APEH-depleted dog liver and renal cytosol prepared by immunodepletion using anti-APEH antiserum completely abolished the VPA-G hydrolytic

activity as well as a typical substrate of APEH. These results demonstrate that cytosolic APEH is a major VPA-G hydrolase in dog liver and kidney as well as in human liver. It is noteworthy that *ex vivo* APEH activity was negligible in dog liver and kidney samples obtained after co-administration with MEPM, and the lack of APEH activity was maintained until 24 h, consistent with a sustainable low level of plasma VPA for several days even after discontinuation of carbapenem in clinical settings. These findings suggest that the DDI of VPA with carbapenems in dogs is caused by the long-lasting inhibition of VPA-G hydrolysis mediated by APEH, resulting in the rapid decrease in plasma VPA levels and an increase in urinary excretion of VPA-G. Furthermore, this study suggests the utility of animal *in vivo* models combined with *in vitro* examinations to identify the involved enzymes for a better understanding of clinical DDI mechanisms.

Section II describes the drug disposition and APEH activity in chimeric mice with humanized livers after co-administration of VPA with MEPM. Similar to the findings in dogs in Section I, chimeric mice with humanized livers showed rapid decrease in plasma VPA, increased urinary excretion of VPA-G and long-lasting inhibition of APEH in humanized liver after co-administration, suggesting the clinical importance of APEH-mediated VPA-G hydrolysis in the DDI mechanism. In addition, hepatic APEH was a major contributor to the DDI since normal mice with intact livers did not show the DDI. Although the plasma $t_{1/2}$ of VPA did not reach that in the clinical setting, chimeric mice with humanized livers are suggested to be a functional tool for assessing the qualitative clinical feasibility of DDIs via a non-P450 enzyme, and for clarifying DDI mechanisms.

Chapter 3 addresses the inhibition mechanism of APEH by carbapenems. Preincubation time-dependent inhibition of VPA-G hydrolysis in human liver cytosol with carbapenems suggests irreversible inhibition of APEH by carbapenems. Purified porcine liver APEH, which showed comparable K_m, the similar chemical inhibition profiles and 92% identity of amino acid sequence with its human counterpart, lacked VPA-G hydrolase activity after incubation with MEPM, and the lacking activity did not recover after overnight dialysis. These observations are consistent with long-lasting inhibition of APEH in dogs and chimeric mice with humanized livers, and the delayed recovery of plasma VPA levels in clinical settings. The irreversible inhibition is primarily explained by the selective binding to the active serine of APEH since preincubation of porcine APEH with DFP, which binds to the active serine of serine proteases, prevented the binding of MEPM to APEH. The open β-lactam ring form of MEPM, clavulanic acid and three penicillins with various sizes of side chains attached to β-lactam ring lacked the inhibitory effect upon VPA-G hydrolysis in human liver cytosol, suggesting that the closed β-lactam ring is essential, and other structural properties unique to carbapenems, such as its non-heterocyclic structure and relative configuration of the side chain of the β-lactam ring, may affect the inhibition.

Concluding Remarks

This thesis investigated the DDI mechanism of VPA with carbapenems based on the hypothesis that the inhibition of reverse hydrolysis to VPA from VPA-G by carbapenems causes the rapid decrease in plasma VPA levels. The important findings of the present work are listed as concluding remarks of this thesis:

1). Cytosolic APEH is a single PAPM-sensitive VPA-G hydrolase in human liver. The involvement of APEH in drug metabolism was shown for the first time. The present work also provides an example that hydrolase is a major enzyme in the catalyzation of the deconjugation of acylglucuronide, which is primarily considered to be mediated by β-glucuronidase.

2). The clinical importance of APEH-mediated VPA-G hydrolysis in the DDI mechanism is suggested through dog *in vitro/in vivo* and chimeric mice with humanized liver *in vivo* examinations. Utility of the animal model used in this work is also suggested.

- Long-lasting inhibition of APEH-mediated VPA-G hydrolysis by MEPM caused the DDI of VPA with MEPM in dogs and chimeric mice with humanized livers, resulting in the rapid decrease in plasma VPA levels and increase in urinary excretion of VPA-G. *In vivo* inhibition of APEH activity after administration of carbapenem was shown for the first time.
- Hepatic APEH was a major contributor to the DDI and renal APEH might be involved in part.
- This work is the first example to show the capability of chimeric mice with humanized livers to evaluate DDIs via a non-P450 enzyme.

3). Carbapenems irreversibly inhibit APEH. The inhibition mechanism is primarily explained by selective binding to the active serine of APEH. The closed β-lactam ring in the carbapenem structure is essential for the inhibition.

Finally, this research will contribute to bringing much attention to safer clinical use of VPA and carbapenems (whose concomitant use is still allowed in the world, except for Japan), through better understanding the DDI mechanism of both drugs. Furthermore, the present work would give us novel scientific knowledge that the inhibition of reverse metabolism could be a cause of the drug interaction, especially in the case that the relevant reverse pathway is converted from a main metabolite to the parent drug mediated by a single enzyme. Moreover, the methodologies used in this research, combination of animal *in vivo* model with *in vitro* examinations including the identification of the responsible enzyme for reverse metabolism, would be widely applicable for future research of reverse metabolism-related DDIs. Thus, the author hopes that these findings will aid in the understanding of unclarified mechanisms of DDI in the future.

Experimental

Chapter 1

1. Materials

VPA-G was synthesized enzymatically in Chemtech Labs, Inc. (Tokyo, Japan). PAPM was synthesized in Sankyo Co., Ltd. (Tokyo, Japan). VPA sodium salt and EDTA were purchased from Sigma Chemical Co. (St. Louis, MO). DFP, eserine, *p*-nitroaniline, pNPG and *p*-nitrophenol were purchased from Wako Pure Chemicals (Osaka, Japan). BNPP and DTNB were purchased from Nacalai Tesque, Inc. (Kyoto, Japan). PCMB and saccharolactone were purchased from Research Organics (Cleveland, OH) and MP Biomedicals, Inc. (Solon, OH), respectively. AANA was purchased from Bachem AG (Bubendorf, Switzerland). The other reagents were all commercially available and of guaranteed grade. Pooled human liver subcellular fractions and human liver tissue used for the purification of VPA-G hydrolase were obtained from XenoTech, LLC. (Lenexa, KS) and Human & Animal Bridging Research Organization (Chiba, Japan). Bovine liver β-glucuronidase was purchased from ProZyme, Inc. (San Leandro, CA).

2. VPA-G Hydrolysis and Inhibition

Either human liver subcellular fraction (cytosol, microsomes, mitochondria and lysosomes; 1 mg/mL each) or recombinant human APEH (0.1 mg/mL) was preincubated in 50 mM Tris-HCl buffer (pH 7.4) at 37°C. Then, VPA-G (30 μM) was added to make a final volume of 0.05 – 0.1 mL and further incubation was performed at 37°C. The reaction was stopped by adding the same volume of acetonitrile containing chlorzoxazone (0.5 – 5 μM, internal standard [IS]) as the reaction mixture and was centrifuged. An aliquot of 10 μL of each supernatant was injected into an LC/MS system. Human liver lysosomes were also incubated in 50 mM sodium acetate buffer (pH 5). In the inhibition studies, either PAPM, β-glucuronidase inhibitor (saccharolactone) or esterase inhibitor (DFP, eserine, BNPP, DTNB, EDTA, and PCMB) was added to the reaction mixture before preincubation. In the β-glucuronidase study, bovine liver β-glucuronidase (200 Fishman unit/mL) was preincubated in 50 mM sodium acetate buffer (pH 5) and further incubation was performed after the addition of VPA-G.

3. Measurement of VPA Concentration

The concentrations of VPA in the incubation samples were analyzed using an LC/MS system consisting of an LC-10A (Shimadzu Corporation, Kyoto, Japan) coupled to an API3000 (Applied Biosystems/MDS SCIEX; Foster City, CA). Chromatographic separation was achieved on a Capcell Pak C18 MG column (5 μm, 2.0 × 150 mm; Shiseido Co., Ltd., Tokyo, Japan) at a column temperature of 40°C. A mixture of acetonitrile/water (5/95, v/v) containing 5 mM ammonium acetate (mobile phase A) and acetonitrile/water (95/5, v/v) containing 5 mM ammonium acetate (mobile phase B) were used at a flow

rate of 0.3 mL/min. The following gradient elution program was used: a linear increase of mobile phase B from 40% to 60% for 4 min followed by elution with 60% mobile phase B for 0.45 min. The eluent from the column was introduced directly to the API3000 using the electrospray ionization interface in negative ion mode. The ions of *m/z* 143 for VPA and *m/z* 168 for IS were monitored using the selected ion monitoring mode. For both VPA and IS, the declustering potential, curtain gas, ion spray voltage and ion source temperature were -31 V, 6 psi, -3,500 V and 550°C, respectively.

4. LDH Activity in Human Liver Subcellular Fractions

The LDH activity in human liver subcellular fractions was measured using an LDH assay kit (L-type Wako LDH, Wako Pure Chemicals) according to the manufacturer's instructions.

5. Purification of VPA-G Hydrolase from Human Liver Cytosol

Human liver tissue was homogenized in a buffer (250 mM sucrose, 3 mM Tris and 1 mM EDTA [pH 7.4]) and the cytosol fraction was prepared by a conventional method. Briefly, the cytosol was fractionated by ammonium sulfate and 20 to 70% (w/v) precipitate was obtained. The precipitate was dissolved in 20 mM HEPES (pH 7) and dialyzed against the same buffer. The dialysate was applied to a HiPrep 16/10 Q FF column (20 mL, GE Healthcare, Uppsala, Sweden) equilibrated with 20 mM HEPES (pH 7) and then a linear gradient of 0 to 0.5 M NaCl was applied to elute the enzyme. The active fractions were combined and dialyzed against 10 mM of potassium phosphate buffer (pH 6.8) containing 0.3 mM $CaCl_2$. The dialysate was applied to a Bio-Scale CHT2-I column (2 mL, Bio-Rad Laboratories, Hercules, CA) and then a linear gradient of 0 to 50% potassium phosphate buffer (500 mM, pH 6.8) containing 0.01 mM $CaCl_2$ was applied to elute the enzyme. After each active fraction was analyzed by SDS-PAGE, a 75-kDa protein band visualized by silver staining (EzStain Silver, ATTO Corporation, Tokyo, Japan) was excised and digested with trypsin within the gel. The resulting peptides were extracted and sequenced by LC/MS/MS, which consisted of a DiNa nano-flow liquid chromatography system (KYA Tech, Tokyo, Japan) and an LTQ Orbitrap (Thermo Fisher Scientific, Waltham, MA). The MS/MS spectra data were searched against a composite target/decoy IPI human database (version 3.72; 172784 forward and reversed protein sequences) using Mascot 2.2 (Matrix Science, London, UK). Parent mass and MS/MS tolerances were set at 50 ppm and 0.8 Da, respectively. The author required strict enzyme specificity and allowed for up to two missed cleavage sites. Carbamidomethylation of cysteine was set as the fix modification, and oxidation of methionine and N-acetylation of protein were searched as variable modifications. The search results were filtered and summarized using in-house developed software. In the software, the estimated false discovery rate of all peptide identifications was fixed at less than 1% by automatically filtering on mass error and peptide score of all forward and reverse peptide identifications.

6. Preparation of Recombinant Human APEH with FLAG Tag

The expression vector, pcDNA-NFLAG-GW, was prepared by Daiichi-Sankyo Co., Ltd. Ultimate ORF Clone (IOH3679, Matching nucleotide accession number: NM_001640.3, Invitrogen

Corporation, Carlsbad, CA), which has an open reading frame of human APEH, was recombined with pcDNA-NFLAG-GW by a Gateway LR reaction. This vector was transfected into FreeStyle 293F cells (Invitrogen) using 293fectin (Invitrogen) according to the manufacturer's instructions. The transfected cells were cultured for 96 h and the harvest was centrifuged. Recombinant APEH in the supernatant was applied to anti-FLAG M2 affinity gel (Sigma) and was eluted with FLAG peptide (Sigma). The eluate was purified using the same procedure as described above.

7. Antiserum and Immunodepletion

A rabbit was immunized 8 times over a period of 3 months by subcutaneous injection of a mixture of recombinant APEH (100 μg) and oil adjuvant (Freund's adjuvant complete [1st immunization only] or Freund's adjuvant incomplete, Difco Laboratories Inc, Detroit, MI). In 7 days after the final immunization, whole blood was collected and anti-APEH antiserum was obtained by centrifugation. Aliquots of 100 μL of Protein G Sepharose 4 Fast Flow beads (GE Healthcare) were washed with 500 μL of TNN.15 buffer (20 mM Tris-HCl [pH 7.4], 150 mM NaCl and 0.1% NP-40) and centrifuged. After discarding the supernatant, the precipitate was suspended in 400 μL of the same buffer. A 50-μL aliquot of the antiserum was applied to the prepared beads and was gently mixed overnight at 4°C to retain the enzyme on the beads. The antiserum binding beads were washed with 500 μL of TNN.15 buffer 3 times, followed by a wash with the same volume of TNN.1 (20 mM Tris-HCl [pH 7.4], 100 mM NaCl and 0.1% NP-40). The beads were suspended with 500 μL of TNN.1. Aliquots of 250 μL of the antiserum binding bead suspension were centrifuged and the supernatant was discarded. To the beads, 40 μL of human liver cytosol and 360 μL of TNN.1 buffer were added and the suspension was mixed gently for 2 h at 4°C. After centrifugation, the supernatant was treated with 250 μL of the bead suspension again. The resulting supernatant obtained after centrifugation was used as APEH depleted cytosol and Western blot analysis was performed to check the depletion of APEH. The various hydrolytic activity in the cytosol was also measured. As a negative control, cytosol was also applied to beads treated with either preimmune serum or TNN.15 buffer.

8. Western Blotting

APEH depleted cytosol (10 μg) was separated by SDS-PAGE and was transferred electrophoretically onto a polyvinylidene difluoride membrane (Immun-Blot PVDF membrane, 0.2 μm, Bio-Rad). APEH protein was detected with anti-APEH antiserum as a primary antibody and ECL anti-rabbit IgG horseradish peroxidase-linked, from donkey (GE Healthcare, 1:1,000,000 dilution) as a secondary antibody. The immunoblots were visualized by chemiluminescence with an ECL Advance Western blotting detection kit (GE Healthcare).

9. APEH Activity

APEH activity in immunodepleted cytosol (0.1 mg/mL) was assayed as described below. Each cytosol was incubated with AANA as a substrate in 100 mM Tris-HCl buffer (pH 7.4) at 37°C. The

formation of *p*-nitroaniline was measured spectrophotometrically by monitoring the increase in absorbance at 405 nm.

10. β-Glucuronidase Activity

β-Glucuronidase activity in immunodepleted cytosol (0.1 mg/mL) was measured as described previously with a little modification [57]. Each cytosol was incubated with pNPG (5 mM) as a substrate in 100 mM sodium acetate buffer (pH 5) or 100 mM Tris-HCl buffer (pH 7.4) at 37°C. The formation of *p*-nitrophenol was measured spectrophotometrically by monitoring the increase in absorbance at 405 nm.

Chapter 2, Section I

1. Materials

The materials stated above (Experimental Chapter 1.1) were used except as otherwise noted. Eserine, BNPP, and saccharolactone were purchased from Sigma-Aldrich Co. (St. Louis, MO). MEPM was synthesized in Chemtech Labs, Inc. or purchased from Sumitomo Pharmaceutical Co. (Osaka, Japan). PCMB and *p*-nitroaniline were purchased from Tokyo Chemical Industries Co., Ltd. (Tokyo, Japan). The other reagents were all commercially available and of guaranteed grade. Pooled dog liver and renal cytosols were obtained from XenoTech, LLC (Lenexa, KS). Individual dog liver and renal subcellular fractions were prepared as described in other literature. Anti-human APEH antisera was obtained from a rabbit in Experimental Chapter 1.7.

2. Animals

Male Beagle dogs (n=3) were obtained from Nosan Corporation (Tokyo, Japan) and LSG Corporation (Tokyo, Japan). The dogs ranged from 3 years to 7 years old and the body weight was 8.8 kg to 11.5 kg. All experimental procedures were performed in accordance with the in-house guidelines of the Institutional Animal Care and Use Committee of Daiichi Sankyo Co., Ltd.

3. Dog *in vivo* Study

This was conducted as a crossover study with a washout period of more than one week. Dogs subjected to common bile duct cannulation were intravenously coadministered 30 mg/kg of VPA and 100 mg/kg of MEPM or physiological saline as the control. Blood was collected at 0.25, 0.5, 1, 1.5, 2, 3, 4 and 6 h after dosing and was centrifuged to obtain the plasma sample. Urine and bile were collected for the periods of 0 to 1, 1 to 2, 2 to 4 and 4 to 6 h after dosing. Plasma, urine, and bile samples were centrifuged after adding acetonitrile containing IS and the VPA and VPA-G concentrations in the supernatant were measured. A liver biopsy sample was collected from one of the dogs at 6 h and 24 h after dosing under thiopental (inductive, 15 – 20 mg/kg) and isoflurane (continuous, 1.0 – 3.5%) anesthesia, maintaining warmth through a heatpad and applying anti-infectious treatments. After a recovery period of two months, the dog was administered VPA and MEPM or saline again and the kidney biopsy sample was collected under the condition described above. The S9 fraction of each sample was prepared as described above.

4. Measurement of VPA and VPA-G Concentrations

In vivo samples were analyzed using an LC-MS/MS system consisting of an LC-10ADvp (Shimadzu Corporation, Kyoto, Japan) coupled to an API4000 (Applied Biosystems/MDS SCIEX; Foster City, CA). Chromatographic separation was achieved on a Capcell Pak C18 MGIII column (5 μm, 2.0 × 50 mm; Shiseido Co., Ltd., Tokyo, Japan) at a column temperature of 50°C. A mixture of water containing 1 mM ammonium acetate (mobile phase A) and acetonitrile/water (95/5, v/v) containing 20 mM

ammonium acetate (mobile phase B) were used at a flow rate of 0.4 ml/min. The following gradient elution program was used: a linear increase of mobile phase B from 5% to 65% for 6 min followed by a linear increase of mobile phase B to 100% for 0.5 min. The eluent from the column was introduced directly to the API4000 using the electrospray ionization interface in negative ion mode. The transitions of m/z 319.0 to 112.9 for VPA-G, m/z 142.9 to 142.9 for VPA and m/z 168.0 to 131.9 for IS were monitored using the multiple reaction monitoring mode.

5. Data Analysis

PK parameters of VPA and VPA-G after administration of VPA to dogs were calculated using Phoenix WinNonlin (version 6.1, Pharsight Corporation) based on a noncompartmental method.

6. Identification of a Dog VPA-G Hydrolase

VPA-G hydrolase activity in dog liver and renal subcellular fraction and the inhibition

Individual dog subcellular fractions (liver or renal cytosol, microsomes, mitochondria, lysosomes and S9; 1 mg/ml each) prepared from two dogs were preincubated in 50 mM Tris-HCl buffer (pH 7.4) at 37°C. Then, VPA-G (30 μM) was added to make a final volume of 0.1 ml and further incubation was performed at 37°C. The reaction was stopped by adding the same volume of acetonitrile containing chlorzoxazone (0.5 μM, IS) as the reaction mixture and was centrifuged. An aliquot of 10 μl of each supernatant was injected into an LC/MS system. Dog liver and renal lysosomes were also incubated in 50 mM sodium acetate buffer (pH 5). In the inhibition studies, either carbapenems or esterase inhibitors were added to the reaction mixture before preincubation. Pooled liver and renal cytosols were used in the inhibition study using esterase inhibitors. The concentrations of VPA in the incubation samples were analyzed using a method described in Experimental Chapter 1. 3.

Immunodepletion.

Aliquots of 100 μl of Protein G Sepharose 4 Fast Flow beads (GE Healthcare) were washed with 500 μl of TNN.15 buffer (20 mM Tris-HCl [pH 7.4], 150 mM NaCl and 0.1% NP-40) and centrifuged. After discarding the supernatant, the precipitate was suspended in 400 μl of the same buffer. A 50-μL aliquot of the antiserum was applied to the prepared beads and was gently mixed overnight at 4°C to retain the enzyme on the beads. The antiserum binding beads were washed with 500 μl of TNN.15 buffer 3 times, followed by a wash with the same volume of TNN.1 (20 mM Tris-HCl [pH 7.4], 100 mM NaCl and 0.1% NP-40). The beads were suspended with 500 μl of TNN.1. Aliquots of 250 μl of the antiserum binding bead suspension were centrifuged and the supernatant was discarded. To the beads, pooled dog liver or renal cytosol (2 – 4 mg/ml) in TNN.1 buffer was added and the suspension was mixed gently for 2 h at 4°C. After centrifugation, the supernatant was treated with 250 μl of the bead suspension again. The resulting supernatant obtained after centrifugation was used as the APEH depleted cytosol. As a negative control, each fraction was also applied to the beads treated with either preimmune serum or TNN.15 buffer.

APEH and β-glucuronidase activity.

APEH and β-glucuronidase activity in the immunodepleted cytosol (0.2 mg/ml) was measured as described in Experimental Chapter 1.9 and 1.10.

Chapter 2, Section II

1. Materials

The materials stated above (Experimental Chapter 1.1 and Chapter 2, Section I.1, respectively) were used except that VPA-G was purchased from Toronto Research Chemicals (Toronto, Canada).

2. Animals

Male chimeric TK-NOG mice with humanized liver prepared at the Central Institute for Experimental Animals (Kanagawa, Japan) and male control TK-NOG mice were obtained from In Vivo Science Inc. (Tokyo, Japan) (body weight 21 – 30 g). In the chimeric mice, more than 70% of liver cells were estimated to have been replaced with human hepatocytes, as judged by measurements of human albumin concentrations in plasma performed by the supplier. All experimental procedures were performed in accordance with the in-house guidelines of the Institutional Animal Care and Use Committee of Daiichi Sankyo Co., Ltd.

3. Mouse *in vivo* Study

The *in vivo* studies using the mice were performed 9 – 14 weeks after transplantation of human hepatocytes. Three control mice and four chimeric mice were intravenously co-administered 30 mg/kg of VPA with 125 mg/kg of MEPM. Three control mice and two chimeric mice were intravenously administered 30 mg/kg of VPA with physiological saline as the control. Blood was collected at 0.25, 0.5, 1, 1.5, 2, 3 and 4 h after dosing and was centrifuged to obtain the plasma sample. After a washout period of two weeks, three control mice and three chimeric mice were co-administered of VPA with MEPM or saline again and urine was collected for the period of 0 to 24 h after dosing. After drawing blood from the heart as much as possible, liver and kidney samples were obtained and were homogenized in a buffer (50 mM Tris-HCl, 0.2 mM EDTA, pH 7.4) of four-fold the volume of tissue weight. The samples were centrifuged at 700 g for 10 min at 4ºC and the supernatant was used as the tissue homogenate. Plasma and urine samples were centrifuged after adding acetonitrile containing IS and the plasma VPA, plasma VPA-G and urinary VPA-G concentrations in the supernatant were measured.

4. Measurement of VPA and VPA-G Concentrations

Plasma and urine samples were analyzed using an LC-MS/MS system consisting of an LC-20AD (Shimadzu Corporation, Kyoto, Japan) coupled to an API4000 (Applied Biosystems/MDS SCIEX; Foster City, CA). Chromatographic separation was achieved on a Capcell Pak C18 MGIII column (5 μm, 2.0 × 50 mm; Shiseido Co., Ltd., Tokyo, Japan) at a column temperature of 50°C. A mixture of water containing 1 mM ammonium acetate (mobile phase A) and acetonitrile/water (95/5, v/v) containing 20 mM ammonium acetate (mobile phase B) were used at a flow rate of 0.4 ml/min. The following gradient elution program was used: a linear increase of mobile phase B from 5% to 65% for 6 min followed by a linear increase of mobile phase B to 100% for 0.5 min. The eluent from the column was introduced

directly to the API4000 using the electrospray ionization interface in negative ion mode. The transitions of m/z 319.0 to 112.9 for VPA-G in plasma, m/z 319.0 to 142.9 for VPA-G in urine, m/z 142.9 to 142.9 for VPA in plasma and m/z 168.0 to 131.9 for IS were monitored using the multiple reaction monitoring mode.

5. Data Analysis

PK parameters of VPA and VPA-G after administration of VPA to mice were calculated using Phoenix WinNonlin (version 6.3, Pharsight Corporation) based on a noncompartmental method.

6. APEH Activity

APEH activity in tissue homogenates was measured as described in Experimental Chapter 1.9 and 1.10.

Chapter 3

1. Materials

The materials stated above (Experimental Chapter 1.1) were used except as otherwise noted. BSA and benzylpenicillin sodium salt were purchased from Sigma-Aldrich Co. (St. Louis, MO). ^{14}C-MEPM was synthesized in Daiichi Pure Chemicals Co., Ltd. (Ibaraki, Japan). The open β-lactam ring form of MEPM was synthesized at Sankyo Co., Ltd. (Tokyo, Japan). Clavulanic acid potassium salt and ampicillin sodium salt were purchased from Wako Pure Chemicals (Osaka, Japan). 6-Aminopenicillanic acid was purchased from Tokyo Chemical Industry Co., Ltd. (Tokyo, Japan). The other reagents were all commercially available and of guaranteed grades. Purified porcine liver APEH was obtained from Takara Bio Inc. (Shiga, Japan).

2. Kinetic Parameters Determination

Human liver cytosol (1 mg/mL) was preincubated in 50 mM Tris-HCl buffer (pH 7.4) at 37°C. Then, the preincubation mixture was incubated with VPA-G (1 – 200 μM) for 15 min at 37°C (the total reaction volume: 0.2 mL). Likewise, purified porcine liver APEH (3.08 μg/mL) was incubated with VPA-G (1 – 30 μM) in 50 mM Tris-HCl buffer (pH 7.4) for 15 min at 37°C (the total reaction volume: 0.4 mL). The reaction was stopped by adding the same volume of acetonitrile containing chlorzoxazone (0.5 – 5 μM, IS) and was centrifuged. VPA concentrations in the supernatant were measured by an LC/MS system consisting of an LC-10A chromatograph (Shimadzu Corporation, Kyoto, Japan) coupled to an API3000 (Applied Biosystems/MDS SCIEX; Foster City, CA) mass spectrometer. Chromatographic separation was achieved on a Capcell Pak C18 MG column (5 μm, 2.0 × 150 mm; Shiseido Co., Ltd., Tokyo, Japan) at a column temperature of 40°C. A mixture of acetonitrile/water (5/95, v/v) containing 5 mM ammonium acetate (mobile phase A) and acetonitrile/water (95/5, v/v) containing 5 mM ammonium acetate (mobile phase B) were used at a flow rate of 0.3 mL/min. The following gradient elution program was used: a linear increase of mobile phase B from 40% to 60% for 4 min followed by elution with 60% mobile phase B for 0.45 min. The eluent from the column was introduced directly to the API3000 using the electrospray ionization interface in negative ion mode. The ions of *m/z* 143 for VPA and *m/z* 168 for IS were monitored using the selected ion monitoring mode. For both VPA and IS, the declustering potential, curtain gas, ion spray voltage and ion source temperature were -31 V, 6 psi, -3,500 V and 550°C, respectively.

3. Enzyme Inhibition

IC_{50} determination.

Various concentrations of PAPM, MEPM or the open ring form of MEPM (0 – 100 μM) were preincubated for 0 to 30 min with human liver cytosol (1 mg/mL) at 37°C. Then the preincubation mixtures were incubated with VPA-G (3 μM, approximately equal to K_m) and the production of VPA was determined.

Effect of other β-lactam antibiotics.

Various concentrations of clavulanic acid, 6-aminopenicillanic acid, benzylpenicillin, ampicillin and MEPM (0 – 200 μM) were preincubated for 10 min with human liver cytosol (1 mg/mL) at 37°C. Then the preincubation mixtures were incubated with VPA-G (30 μM) and the production of VPA was determined.

4. Effect of Dialysis

Inhibition of VPA-G hydrolysis.

Purified porcine liver APEH (0.5 nmol), MEPM (0.5 nmol) and Tris-HCl Buffer (50 mM, pH 7.4) were mixed (final volume 800 μL) and were incubated for 1 h at 37°C. The reaction mixture was transferred into dialysis cassette (Slide-A-Lyzer Dialysis Cassette, 3.5K molecular weight cut-off, 0.5 – 3.0 mL capacity, Pierce Biotechnology Inc., Rockford, IL) and was dialyzed twice against 300 mL of 50 mM Tris-HCl at 4°C for 3 h and overnight, respectively. APEH incubated without MEPM was also subjected to dialysis. The VPA-G hydrolytic activity in the reaction mixture before and after dialysis was measured. The inhibition ratio of activity was calculated by dividing the activity of APEH with incubation with MEPM by that with incubation without MEPM.

Binding of MEPM to APEH.

To examine the binding of MEPM to APEH, another dialysis experiment was performed using ^{14}C-MEPM according to the same procedure as described above. The radioactivity in the dialysate was divided by the initial radioactivity in the reaction mixture to calculate the binding ratio of ^{14}C-MEPM to APEH. To check the binding specificity of MEPM, the binding ratio to BSA was also examined.

Effect of DFP on binding of MEPM to APEH.

Porcine APEH was preincubated with DFP (0.5 nmol) for 30 min at 37°C and then was incubated with ^{14}C-MEPM for 1 h. The binding ratio was determined using the same procedure as described above. To check the non-specific effect of DFP, the binding ratio of MEPM to BSA after preincubation with DFP was examined.

5. Data Analysis

K_m and V_{max} for VPA-G hydrolysis in human liver cytosol were calculated using WinNonlin Professional (version 4.0.1, Pharsight Corporation) based on a pharmacodynamic compiled model (simple E_{max} model, model No. 101). IC_{50} values of carbapenems were calculated using WinNonlin based on a pharmacodynamic compiled model (inhibitory effect sigmoid E_{max} model, model No. 107).

References

1. Leucuta SE and Vlase L. Pharmacokinetics and metabolic drug interactions. *Curr Clin Pharmacol* **1:**5-20 (2006)
2. Kennedy DT, Hayney MS, Lake KD. Azathioprine and allopurinol: the price of an avoidable drug interaction. *Ann Pharmacother* **30:**951-4 (1996)
3. Diasio RB. Sorivudine and 5-fluorouracil; a clinically significant drug-drug interaction due to inhibition of dihydropyrimidine dehydrogenase. *Br J Clin Pharmacol* **46:**1-4 (1998)
4. Williams ET, Carlson JE, Lai WG, Wong YN, Yoshimura T, Critchley DJ, Narurkar M. Investigation of the metabolism of rufinamide and its interaction with valproate. *Drug Metab Lett* **5:**280-9 (2011)
5. Gnann JW, Jr., Crumpacker CS, Lalezari JP, Smith JA, Tyring SK, Baum KF, Borucki MJ, Joseph WP, Mertz GJ, Steigbigel RT, Cloud GA, Soong SJ, Sherrill LC, DeHertogh DA, Whitley RJ. Sorivudine versus acyclovir for treatment of dermatomal herpes zoster in human immunodeficiency virus-infected patients: results from a randomized, controlled clinical trial. Collaborative Antiviral Study Group/AIDS Clinical Trials Group, Herpes Zoster Study Group. *Antimicrob Agents Chemother* **42:**1139-45 (1998)
6. Jaiswal S, Sharma A, Shukla M, Vaghasiya K, Rangaraj N, Lal J. Novel pre-clinical methodologies for pharmacokinetic drug-drug interaction studies: spotlight on "humanized" animal models. *Drug Metab Rev* **46:**475-93 (2014)
7. Hasegawa M, Kawai K, Mitsui T, Taniguchi K, Monnai M, Wakui M, Ito M, Suematsu M, Peltz G, Nakamura M, Suemizu H. The reconstituted 'humanized liver' in TK-NOG mice is mature and functional. *Biochem Biophys Res Commun* **405:**405-10 (2011)
8. Yoshizato K and Tateno C. In vivo modeling of human liver for pharmacological study using humanized mouse. *Expert Opin Drug Metab Toxicol* **5:**1435-46 (2009)
9. de Jong YP, Rice CM, Ploss A. New horizons for studying human hepatotropic infections. *J Clin Invest* **120:**650-3 (2010)
10. Nishimura T, Hu Y, Wu M, Pham E, Suemizu H, Elazar M, Liu M, Idilman R, Yurdaydin C, Angus P, Stedman C, Murphy B, Glenn J, Nakamura M, Nomura T, Chen Y, Zheng M, Fitch WL, Peltz G. Using chimeric mice with humanized livers to predict human drug metabolism and a drug-drug interaction. *J Pharmacol Exp Ther* **344:**388-96 (2013)
11. Yamazaki H, Suemizu H, Murayama N, Utoh M, Shibata N, Nakamura M, Guengerich FP. In vivo drug interactions of the teratogen thalidomide with midazolam: heterotropic cooperativity of human cytochrome P450 in humanized TK-NOG mice. *Chem Res Toxicol* **26:**486-9 (2013)
12. Rimmer EM and Richens A. An update on sodium valproate. *Pharmacotherapy* **5:**171-84 (1985)
13. Yamamura N, Imura K, Naganuma H, Nishimura K. Panipenem, a carbapenem antibiotic, enhances the glucuronidation of intravenously administered valproic acid in rats. *Drug Metab Dispos* **27:**724-30 (1999)
14. Cloyd JC, Kriel RL, Fischer JH. Valproic acid pharmacokinetics in children. II. Discontinuation of concomitant antiepileptic drug therapy. *Neurology* **35:**1623-7 (1985)
15. Perucca E. Pharmacological and therapeutic properties of valproate: a summary after 35 years of clinical experience. *CNS Drugs* **16:**695-714 (2002)
16. Levy RH, Rettenmeier AW, Anderson GD, Wilensky AJ, Friel PN, Baillie TA, Acheampong A, Tor J, Guyot M, Loiseau P. Effects of polytherapy with phenytoin, carbamazepine, and stiripentol on formation of 4-ene-valproate, a hepatotoxic metabolite of valproic acid. *Clin Pharmacol Ther* **48:**225-35 (1990)
17. Nagai K, Shimizu T, Togo A, Takeya M, Yokomizo Y, Sakata Y, Matsuishi T, Kato H. Decrease in serum levels of valproic acid during treatment with a new carbapenem, panipenem/betamipron. *J Antimicrob Chemother* **39:**295-6 (1997)
18. De Turck BJ, Diltoer MW, Cornelis PJ, Maes V, Spapen HD, Camu F, Huyghens LP. Lowering of plasma valproic acid concentrations during concomitant therapy with meropenem and amikacin. *J Antimicrob Chemother* **42:**563-4 (1998)
19. Zhanel GG, Wiebe R, Dilay L, Thomson K, Rubinstein E, Hoban DJ, Noreddin AM, Karlowsky JA. Comparative review of the carbapenems. *Drugs* **67:**1027-52 (2007)
20. El-Gamal MI and Oh CH. Current status of carbapenem antibiotics. *Curr Top Med Chem* **10:**1882-97 (2010)
21. Lunde JL, Nelson RE, Storandt HF. Acute seizures in a patient receiving divalproex sodium after starting ertapenem therapy. *Pharmacotherapy* **27:**1202-5 (2007)
22. Haroutiunian S, Ratz Y, Rabinovich B, Adam M, Hoffman A. Valproic acid plasma concentration

decreases in a dose-independent manner following administration of meropenem: a retrospective study. *J Clin Pharmacol* **49:**1363-9 (2009)
23. Taha FA, Hammond DN, Sheth RD. Seizures from valproate-carbapenem interaction. *Pediatr Neurol* **49:**279-81 (2013)
24. Shihyakugari A, Miki A, Nakamoto N, Satoh H, Sawada Y. First case report of suspected onset of convulsive seizures due to co-administration of valproic acid and tebipenem. *Int J Clin Pharmacol Ther* **53:**92-6 (2015)
25. Gu J and Huang Y. Effect of concomitant administration of meropenem and valproic acid in an elderly Chinese patient. *Am J Geriatr Pharmacother* **7:**26-33 (2009)
26. Mori H, Takahashi K, Mizutani T. Interaction between valproic acid and carbapenem antibiotics. *Drug Metab Rev* **39:**647-57 (2007)
27. Kojima S, Nadai M, Kitaichi K, Wang L, Nabeshima T, Hasegawa T. Possible mechanism by which the carbapenem antibiotic panipenem decreases the concentration of valproic acid in plasma in rats. *Antimicrob Agents Chemother* **42:**3136-40 (1998)
28. Torii M, Takiguchi Y, Saito F, Izumi M, Yokota M. Inhibition by carbapenem antibiotic imipenem of intestinal absorption of valproic acid in rats. *J Pharm Pharmacol* **53:**823-9 (2001)
29. Nakajima Y, Mizobuchi M, Nakamura M, Takagi H, Inagaki H, Kominami G, Koike M, Yamaguchi T. Mechanism of the drug interaction between valproic acid and carbapenem antibiotics in monkeys and rats. *Drug Metab Dispos* **32:**1383-91 (2004)
30. Omoda K, Murakami T, Yumoto R, Nagai J, Maeda Y, Kiribayashi Y, Takano M. Increased erythrocyte distribution of valproic acid in pharmacokinetic interaction with carbapenem antibiotics in rat and human. *J Pharm Sci* **94:**1685-93 (2005)
31. Yamamura N, Imura-Miyoshi K, Naganuma H. Panipenum, a carbapenem antibiotic, increases the level of hepatic UDP-glucuronic acid in rats. *Drug Metab Dispos* **28:**1484-6 (2000)
32. Nakamura Y, Nakahira K, Mizutani T. Decreased valproate level caused by VPA-glucuronidase inhibition by carbapenem antibiotics. *Drug Metab Lett* **2:**280-5 (2008)
33. Raphel V, Giardina T, Guevel L, Perrier J, Dupuis L, Guo XJ, Puigserver A. Cloning, sequencing and further characterization of acylpeptide hydrolase from porcine intestinal mucosa. *Biochim Biophys Acta* **1432:**371-81 (1999)
34. Perrier J, Durand A, Giardina T, Puigserver A. Catabolism of intracellular N-terminal acetylated proteins: involvement of acylpeptide hydrolase and acylase. *Biochimie* **87:**673-85 (2005)
35. Scaloni A, Barra D, Jones WM, Manning JM. Human acylpeptide hydrolase. Studies on its thiol groups and mechanism of action. *J Biol Chem* **269:**15076-84 (1994)
36. Giardina T, Biagini A, Massey-Harroche D, Puigserver A. Distribution and subcellular localization of acylpeptide hydrolase and acylase I along the hog gastro-intestinal tract. *Biochimie* **81:**1049-55 (1999)
37. Yokogawa K, Iwashita S, Kubota A, Sasaki Y, Ishizaki J, Kawahara M, Matsushita R, Kimura K, Ichimura F, Miyamoto K. Effect of meropenem on disposition kinetics of valproate and its metabolites in rabbits. *Pharm Res* **18:**1320-6 (2001)
38. Soars MG, Riley RJ, Findlay KA, Coffey MJ, Burchell B. Evidence for significant differences in microsomal drug glucuronidation by canine and human liver and kidney. *Drug Metab Dispos* **29:**121-6 (2001)
39. Kamimura H, Ito S, Nozawa K, Nakamura S, Chijiwa H, Nagatsuka S, Kuronuma M, Ohnishi Y, Suemizu H, Ninomiya S. Formation of the accumulative human metabolite and human-specific glutathione conjugate of diclofenac in TK-NOG chimeric mice with humanized livers. *Drug Metab Dispos* **43:**309-16 (2015)
40. Miyaguchi T, Suemizu H, Shimizu M, Shida S, Nishiyama S, Takano R, Murayama N, Yamazaki H. Human urine and plasma concentrations of bisphenol A extrapolated from pharmacokinetics established in in vivo experiments with chimeric mice with humanized liver and semi-physiological pharmacokinetic modeling. *Regul Toxicol Pharmacol* **72:**71-6 (2015)
41. Yoshida H, Hirozane K, Kimoto H, Hayashi T, Akiyama T, Katayama H, Watanabe M, Yoshitomi H, Kamiya A. Valproic acid elimination rate and urinary excretion of its glucuronide conjugate in patients with epilepsy. *Biol Pharm Bull* **22:**716-20 (1999)
42. Yamamura N, Mueller J, Hoepner U, Roos-Poppe U, Miyoshi K, Naganuma H, Ikeda T. Metabolism-based drug interaction between valproic acid and carbapenem antibiotics. *6th International ISSX Meeting* (2001)
43. Thomas MH, Dash CH, Burnand KG, Woodyer AB. The excretion of cefuroxime in human bile. *Br J Surg* **68:**290-1 (1981)
44. Shiramatsu K, Hirata K, Yamada T, Kimura H, Someya T, Usuki T, Karasawa G, Hayasaka H. Ceftazidime concentration in gallbladder tissue and excretion in bile. *Antimicrob Agents Chemother* **32:**1588-9 (1988)

45. Morimoto K, Kinoshita H, Nakatani S, Sakai K, Fujimoto M, Ohno K, Ueda T, Hirata S, Muramatsu H, Mizugami K, Morimoto Y, Ohmori K. Panipenem/betamipron in the treatment of patients with surgical infections. *Jpn J Chemother* **39 Suppl 3:**572-584 (1991)
46. Granai F, Smart HL, Triger DR. A study of the penetration of meropenem into bile using endoscopic retrograde cholangiography. *J Antimicrob Chemother* **29:**711-8 (1992)
47. Yamagata T, Momoi MY, Murai K, Ikematsu K, Suwa K, Sakamoto K, Fujimura A. Panipenem-betamipron and decreases in serum valproic acid concentration. *Ther Drug Monit* **20:**396-400 (1998)
48. Mitta M, Ohnogi H, Mizutani S, Sakiyama F, Kato I, Tsunasawa S. The nucleotide sequence of human acylamino acid-releasing enzyme. *DNA Res* **3:**31-5 (1996)
49. Masuo Y, Ito K, Yamamoto T, Hisaka A, Honma M, Suzuki H. Characterization of inhibitory effect of carbapenem antibiotics on the deconjugation of valproic acid glucuronide. *Drug Metab Dispos* **38:**1828-35 (2010)
50. Drawz SM and Bonomo RA. Three decades of beta-lactamase inhibitors. *Clin Microbiol Rev* **23:**160-201 (2010)
51. Casida JE and Quistad GB. Organophosphate toxicology: safety aspects of nonacetylcholinesterase secondary targets. *Chem Res Toxicol* **17:**983-98 (2004)
52. Yamashita N, Kawashima K, Nomura K, Takeuchi H, Watanabe T, Naruke T. Pharmacokinetics of [14C]biapenem in rats. *Chemotherapy (Tokyo).* **42 Suppl 4:**251-267 (1994)
53. Kahan JS, Kahan FM, Goegelman R, Currie SA, Jackson M, Stapley EO, Miller TW, Miller AK, Hendlin D, Mochales S, Hernandez S, Woodruff HB, Birnbaum J. Thienamycin, a new beta-lactam antibiotic. I. Discovery, taxonomy, isolation and physical properties. *J Antibiot (Tokyo)* **32:**1-12 (1979)
54. Roy AB and Hewlins MJ. On the reactions of the carbapenem, meropenem, in the soluble fraction of rat kidney. *Xenobiotica* **24:**185-98 (1994)
55. Sumita Y, Fukasawa M, Mitsuhashi S, Inoue M. Binding affinities of beta-lactam antibodies for penicillin-binding protein 2' in methicillin-resistant staphylococcus aureus. *J Antimicrob Chemother* **35:**473-81 (1995)
56. Lu WP, Kincaid E, Sun Y, Bauer MD. Kinetics of beta-lactam interactions with penicillin-susceptible and -resistant penicillin-binding protein 2x proteins from Streptococcus pneumoniae. Involvement of acylation and deacylation in beta-lactam resistance. *J Biol Chem* **276:**31494-501 (2001)
57. Akao T and Kobashi K. Glycyrrhizin beta-D-glucuronidase of Eubacterium sp. from human intestinal flora. *Chem Pharm Bull (Tokyo)* **35:**705-10 (1987)

Papers in Publication

This thesis is comprised of the following published papers:

1. Suzuki E, Yamamura N, Ogura Y, Nakai D, Kubota K, Kobayashi N, Miura S, Okazaki O. Identification of valproic acid glucuronide hydrolase as a key enzyme for the interaction of valproic acid with carbapenem antibiotics. *Drug Metab Dispos* **38:**1538-1544 (2010)

2. Suzuki E, Nakai D, Ikenaga H, Fusegawa K, Goda R, Kobayashi N, Kuga H, Izumi T. In vivo inhibition of acylpeptide hydrolase by carbapenem antibiotics causes the decrease of plasma concentration of valproic acid in dogs. *Xenobiotica* **46:**126-131 (2016)

3. Suzuki E, Koyama K, Nakai D, Goda R, Kuga H, Chiba K. Observation of clinically relevant drug interaction in chimeric mice with humanized livers: the case of valproic acid and carbapenem antibiotics. *Eur J Drug Metab Pharmacokinet.* doi: 10.1007/s13318-017-0413-2

4. Suzuki E, Nakai D, Yamamura N, Kobayashi N, Okazaki O, Izumi T. Inhibition mechanism of carbapenem antibiotics on acylpeptide hydrolase, a key enzyme in the interaction with valproic acid. *Xenobiotica* **41:**958-963 (2011)

Acknowledgements

The author would like to extend her sincere appreciation to Prof. Dr. Kan Chiba, Laboratory of Pharmacology & Toxicology, Graduate School of Pharmaceutical Sciences, Chiba University, who offered invaluable guidance, thoughtful discussions, and continuous support throughout the work on this thesis.

This research has been carried out in Drug Metabolism and Pharmacokinetics Research Laboratories, Daiichi Sankyo Co., Ltd. The author wishes to express her gratitude to Dr. Osamu Ando, Vice President of Drug Metabolism and Pharmacokinetics Research Laboratories, as well as Dr. Takashi Izumi, the former Vice President of Drug Metabolism and Pharmacokinetics Research Laboratories, for giving her the opportunity to work on the research and providing positive support. The author is especially grateful to Dr. Daisuke Nakai who provided many constructive discussions, professional guidance, and continuous encouragement for her to proceed on the research and publications. Special gratitude is due to Dr. Naotoshi Yamamura for his direction at the beginning of this research; this thesis would not have been possible without his background researches. The author also wishes to thank Drs. Hiroshi Kuga, Nobuhiro Kobayashi, and Shin-ichi Miura for their contributions in participating in productive discussions, and the other members of the research laboratories who kindly supported this work. The author is also thankful to Dr. Osamu Okazaki, previously Vice President of Drug Metabolism and Pharmacokinetics Research Laboratories, Daiichi Sankyo. Co., Ltd. and currently at the Japan Health Sciences Foundation, for his knowledge and assistance.

The author would like to place on record her heartfelt thanks to the following colleagues: Drs. Yuji Ogura and Kazuishi Kubota deserve special thanks for their expert advice on enzyme purification and kind support especially for the author's first publication; Keiichi Fusegawa, Dr. Hidenori Ikenaga and Dr. Kumiko Koyama for their great and thoughtful contributions to conducting dog and chimeric mice with humanized livers *in vivo* studies; Dr. Ryoya Goda for his contribution to bioanalytical method establishment and the successful operations which continuously supported the advance of this research; as well as those who also provided their knowledge, expertise, and assistance with this work.

The author also expresses sincere thanks to her family members and friends for their unconditional support and friendship. Finally, the author is happy to dedicate this thesis to both her daughter and husband, whose familial support has led to the successful completion of the thesis.

Reviewers

This work, for the Degree of Doctor of Pharmaceutical Sciences, was examined by the following reviewers who were authorized by Graduate School of Pharmaceutical Sciences, Chiba University.

Chief reviewer:
Kan Chiba, Ph.D., Professor of Chiba University
(Graduate School of Pharmaceutical Sciences)

Reviewer:
Naoto Yamaguchi, Ph.D., Professor of Chiba University
(Graduate School of Pharmaceutical Sciences)

Reviewer:
Toshihiko Toida, Ph.D., Professor of Chiba University
(Graduate School of Pharmaceutical Sciences)

Reviewer:
Akihiro Hisaka, Ph.D., Professor of Chiba University
(Graduate School of Pharmaceutical Sciences)

Reviewer:
Kousei Ito, Ph.D., Professor of Chiba University
(Graduate School of Pharmaceutical Sciences)